Spring 5-9-2020

Elucidating the Functional Location of Platelet-Derived Growth Factor Receptor Alpha, Creation of a Review Chapter on the use of Zebrafish in Studying Congenital Heart Defects, and using 3D Printing to Create Laboratory Tools

Jaret Lieberth

Elucidating the Functional Location of *platelet-derived growth factor receptor alpha,* Creation of a Review Chapter on the use of Zebrafish in Studying Congenital Heart Defects, and Using 3D Printing to Create Laboratory Tools

By:

Jaret Lieberth

A thesis submitted to the faculty of the University of Mississippi in partial fulfillment of the requirements of the Sally McDonnell Barksdale Honors College.

Oxford, MS

May 2020

Approved by

Dr. Joshua Bloomekatz

Dr. Jennifer Meyer

Dr. Mika Jekabsons

ACKNOWLEDGEMENTS

I would like to extend my sincerest thanks to Dr. Josh Bloomekatz, Dr. Tess McCann, and Rabina Shrestha. Firstly, I'd like to thank Dr. Bloomekatz, my thesis advisor and mentor for these past two and a half years. The work I've had the opportunity to conduct in the Bloomekatz lab has introduced me to the incredibly exciting research potential that zebrafish possess as a model organism, and reshaped career goals which I previously thought concrete. Through your guidance I've been able to grow not only as a student, but as a scientist. Thank you for taking the time to be an amazing mentor, helping me when necessary but still allowing for independent development. To Tess and Rabina, thank you for always having the answers to my questions, and providing the insight and friendship that made everyday work in the lab both possible and enjoyable. Without both of your assistance, I'm sure this project would not have been possible.

I would also like to thank Joseph Natalizio, Savanna Tillman, and Luci Strong. Time in the lab was always made better by each of your presence, and oftentimes our conversations would be the highlights to days when my project felt stuck.

To my second reader, Dr. Jennifer Meyer, I would like to say thank you for being a phenomenal physics instructor, supplemental instruction mentor, and thesis guide, all of which have had positive impacts on my time at Ole Miss. To my third reader, Dr. Mika Jekabsons, thank you for taking the time to work with me towards creating my thesis in a way that reflects the work I've put into it.

Additionally, I would like to extend my thanks to Aurora High School for preparing me for the challenges that my undergraduate career had in store. In particular I would like to thank Mrs. Taylor, whose lessons in writing I still carry with me today.

Lastly, I would like to thank my parents, David and Kristin Lieberth, and the rest of my family, DJ, Jessy, and Whitney. All of you have talked me through moments of stress and uncertainty more than once and for that I am forever grateful, especially considering it was usually at three in the morning. Without the strength, support, and encouragement I received from each of you, I would not be the person I am today.

“Every moral deed and every physical action in a human life are connected in the human heart. We will find the true fusion of these parallel and independent phenomena, moral events, and physical events, only when we truly learn to understand the configuration of the human heart.”

Peter Selg – The Mystery of the Heart

ABSTRACT

Congenital heart defects (CHDs) are currently the most prevalent form of birth defect in the United States. Their combined frequency and severity make necessary a deeper understanding of the molecular underpinnings guiding heart formation. The first major step in cardiac morphogenesis, cardiac fusion, involves the medial movement of bilateral populations of myocardial precursor cells to the embryonic midline, where they merge to form the primitive heart tube. Although crucial to subsequent organogenesis, the precise mechanisms governing cardiac fusion remain unknown. Previous studies have found that a mutation in *platelet-derived growth factor receptor alpha (pdgfra)*, called *refuse-to-fuse (ref)*, results in a lack of proper cardiac fusion in both mouse and zebrafish, implying a regulatory role for *pdgfra* in cardiac fusion. However, the specific tissue that *pdgfra* functions within (myocardium, endocardium, or endoderm) remains unknown. This study details the creation of two transgenic constructs by means of the Gateway multi-site recombination system, Tg(*Bact:loxp-BFP-loxp-Ra-2a-mcherry*) and Tg(*Nkx2.5:Cre-pA*) for the purpose of elucidating the functional location of *pdgfra* during cardiac fusion. These constructs will allow *pdgfra* to be expressed in either the myocardium, endocardium, or endoderm, in mutant *ref* embryos. Thus, allowing us to test whether *pdgfra* expression in the myocardium, endocardium, or endoderm, can rescue the *ref* mutant phenotype. In addition to work identifying the functional location of *pdgfra*, another project undertaken during my time in the Bloomekatz lab involved the creation of a review chapter, covering the use of zebrafish as a model organism to study CHDs. In this endeavor three figures were created, depicting the molecular contractile mechanisms in a sarcomere, an example of zebrafish being used to model a genetic disease involving the gene *titin (ttn)*, and the physiological similarities shared between humans and zebrafish. The review chapter has been accepted and is pending publication. Lastly, my work in the Bloomekatz lab involved multiple 3D printing projects to create confocal microscope slide holders, a feeding gun apparatus, and gel electrophoresis combs.

TABLE OF CONTENTS

LIST OF FIGURES & TABLES

LIST OF ABBREVIATIONS

CHD: Congenital Heart Defect

ALPM: Anterior Lateral Plate Mesoderm

MET: Mesenchymal-to-Epithelial Transition

PDGF: Platelet Derived Growth Factor

RTK: Receptor Tyrosine Kinase

EMT: Epithelial-to-Mesenchymal Transition

pdgfra: Platelet-Derived Growth Factor Receptor Alpha (gene)

VSD: Ventricular Septal Defect

TAPVR: Total Anomalous Pulmonary Venous Return

ref: Refuse-to-Fuse (mutation)

DCM: Dilated Cardiomyopathy

HCM: Hypertrophic Cardiomyopathy

TTNtv: Titin Truncating Variant

ECG: Electrocardiogram

Att Site: Attachment Site

MCS: Multiple Cloning Site

PCR: Polymerase Chain Reaction

BFP: Blue Fluorescent Protein

CFP: Cyan Fluorescent Protein

ttn: titin (gene)

pik: pickwick (mutation)

tnnt2a: Troponin T Type 2a (gene)

sih: Silent-Heart (mutation)

myh6: Myosin Heavy Chain 6 (gene)

myh7: Myosin Heavy Chain 7 (gene)

I. Elucidating the functional tissue location of *platelet-derived growth factor receptor alpha* in cardiac fusion.

1.0: INTRODUCTION

The organogenesis of the mature heart is a complex process involving the coordinated movement of precursor cells and proper communication with neighboring tissues. In the same way that a building cannot be constructed without first laying the correct foundation, the mature heart cannot be formed without first completing early foundational processes. The serial nature of these processes means that the earliest formative steps are of vital importance. Early defects can be compounded throughout the remainder of the heart's formation and cause malformations. One of these early processes involves the medial movement of populations of myocardial precursor cells from their bilateral locations of specification towards the embryonic midline, where they merge in a process termed cardiac fusion (FIGURE 1) [3, 4].

Cardiac fusion is a crucial first step in the formation of the mature heart, as evidenced by the fact that it is evolutionarily conserved in all vertebrates [5]. The process begins with two bilateral populations of cardiac precursor cells in the anterior lateral plate mesoderm (ALPM). Each population is split into endocardial and myocardial precursors. The endocardial precursors move first towards the embryonic midline, followed by the medial movement of the myocardial precursor population and the ALPM [6, 7]. During their movement to the midline, the myocardial precursors undergo a mesenchymal-to-epithelial (MET) transition [8, 9]. During this transition cells convert from a mesenchymal morphology, without cell-to-cell contacts, to an epithelial morphology, exhibiting apical basal polarity and cell-to-cell adhesion [10]. Once migration to the

midline and MET has occurred cells form an epithelial ring covered by an endocardial sheet. Further development and deformation of this simple structure eventually leads to the creation of a two-layered lumen, which gives rise to the primitive heart tube.

Although the importance of cardiac fusion is clear, the underlying mechanisms are unknown. For example, the driver of the movement of the bilateral populations of precursor cells to the midline is unknown. Possible answers to these questions could lie in the interaction between the mesoderm (the aforementioned myocardial and endocardial populations) and the endoderm. Before the migration of either of the mesodermal populations, the myocardial precursors are situated laterally to the adjacent endoderm. When migration towards the embryonic midline first begins, the endodermal and myocardial populations move in a correlated medial manner [12, 13]. However, in the later stages of cardiac fusion the cardiac cells migrate underneath the endoderm, at which point the movement of the two populations is no longer correlated [12, 13]. The related movement of the two populations to the midline, though, suggests a possible role for the endoderm during cardiac fusion. Additionally, previous studies have shown that various mutations affecting endoderm development and specification result in defects in cardiac fusion [14, 15]. The endoderm undoubtedly has a regulatory role in cardiac fusion, but the exact nature of that role remains an unanswered question.

Models have been created, based on correlative studies of endodermal and myocardial movement, which indicate three possible regulatory roles for the endoderm during cardiac fusion. The first possible role is that of a substrate, in which cardiac cells assume an entirely active role and the endoderm functions passively, like a track for the myocardial precursors to move along [16]. The second possible role is that of a cytokine

provider, in which factors provided by the endoderm are responsible for inducing the active movement of myocardial precursors [17]. The final possible role is that of a mechanical force, utilizing cytoskeletal contraction to actively pull the myocardial precursors to the embryonic midline [13]. Data revealing a novel role for the platelet derived growth factor (PDGF) signaling pathway in myocardial precursor movement to the midline [18] may help to identify which of these models is correct.

Platelet-derived growth factors (PDGFs) utilize tyrosine kinase receptors to initiate intracellular signaling cascades [19]. These receptor tyrosine kinases (RTKs) have been shown to play regulatory roles in a plethora of cellular activities such as cell proliferation, survival, adhesion, and differentiation. Furthermore, PDGFs are well studied for their roles as directors of mesenchymal cell migration [20]. Notably, PDGF signaling through RTKs has been implicated in cardiac organogenesis, including in the contribution of cardiac neural crest cells to the outflow tract [21, 22], inflow tract formation, [23], and epicardial epithelial-to-mesenchymal transitions (EMTs) leading to epicardial derivatives [24]. Furthermore, PDGFs play significant roles in the development of congenital heart defects (CHDs). Genetic studies have shown that loss-of-function alleles in platelet-derived growth factor receptor alpha (*pdgfra*) play important roles in the development of many CHDs, including ventricular septal defects (VSDs) and total anomalous pulmonary venous return (TAPVR) [23, 25].

Additionally, recent investigations have shown that zebrafish embryos possessing a loss-of-function mutation in *pdgfra* known as refuse-to-fuse (*ref*) display an early defect in heart tube assembly [18]. These *ref* mutants exhibit a lack of coordinated myocardial cell movement during cardiac fusion and ultimately dysmorphic hearts. This early defect

suggests that CHDs found in *pdgfra* mutant embryos could be the result of a disruption of proper heart tube formation, as well as later cardiac functions. Moreover, it implies that *pdgfra* plays a significant role in heart tube formation. However, it is unknown which tissue *pdgfra* functions within to regulate heart tube formation.

Previous studies performed by the Bloomekatz laboratory, using *in situ* hybridization to visualize *pdgfra* expression in zebrafish embryos, revealed a strong pattern of expression in the ALPM [18]. Because the ALPM is where cardiomyocyte precursor cells are located, **we hypothesize that *pdgfra* functions within cardiomyocyte precursor cells to regulate cardiac fusion**. However, it is additionally possible that *pdgfra* is expressed below the level of detection in other tissues, meaning that a role for *pdgfra* could be discovered in the endoderm or the endocardium. This is within reason, due to the fact that both tissues have been shown to play a role in cardiac fusion [7, 15].

In order to test our hypothesis and determine the functional tissue location of *pdgfra*, our goal is to express *pdgfra* in specific tissues in *ref* mutants and see if the *ref* mutant phenotype is rescued. We are utilizing the Cre/loxP system, which has been previously shown to be effective in zebrafish studies [26]. The Cre/loxP system was chosen as opposed to the similar Gal4/UAS system because the Gal4/UAS system has been shown to be susceptible to epigenetic silencing [27]. Additionally, the Gal4/UAS system has been reported to exhibit mosaic expression through plasmid injection, and a complete expression is crucial for our purposes [28].

The Cre/loxP system is a genetic tool used in animal models in order to control the expression of a gene, spatially or temporally (FIGURE 2). The system is comprised of

two components: a Cre recombinase and loxP recognition sites. In tissues where Cre is present it induces recombination at loxP recognition sites, resulting in the excision of both the loxP sites and the genetic element they are flanking [29]. Our experiment scheme involves four transgenic constructs (FIGURE 3). The first of these transgenic constructs contains a ubiquitous promoter (beta actin) which will drive expression of a gene in every tissue type, loxP sites flanking a fluorescent marker and stop codon, and *pdgfra* downstream (Figure 6B). In tissues where Cre is selectively expressed, recombination occurs between loxP sites, permitting *pdgfra* to be expressed. The other three transgenic constructs allow the tissue-specific expression of Cre. All three are comprised of a tissue-specific promoter for either the myocardium (Nkx2.5), endocardium (flk1), or endoderm (sox17), upstream of a *Cre* element. These constructs will be used in *ref* mutants, which inherently have *pdgfra* expressed in none of their tissues, to ensure that *pdgfra* is expressed only in the desired tissues. As was discovered in our previous study, the *ref* phenotype is characterized by bilateral populations of cardiac progenitor cells, or a horseshoe-shaped population of cardiac progenitor cells, instead of a ring of cardiomyocytes at the midline. During the assay portion of our experimentation, *ref* mutants carrying the Cre/loxP transgenes will be analyzed using fluorescence microscopy and *insitu* hybridization in order to determine which tissue-specific Cre-expressing line displays a rescue of the *ref* phenotype. A complete rescue will be characterized by a single, ring-shaped population of cardiac progenitor cells at the embryonic midline, as is expected during typical cardiac fusion (FIGURE 4).

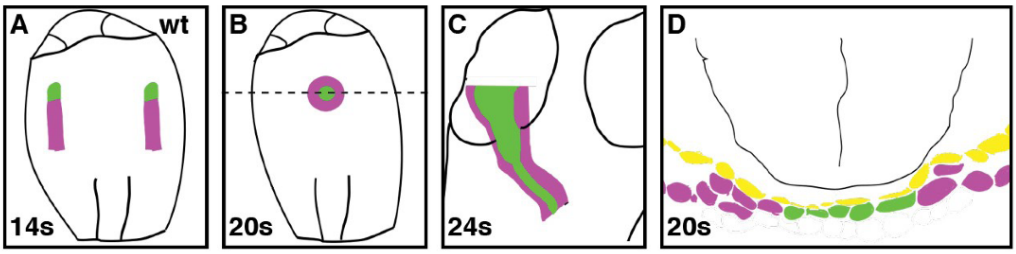

Figure 1: Schematic of Heart Tube Assembly in Zebrafish
(A-C) The formation of the heart tube begins with a process termed cardiac fusion. This process begins with the medial movement of myocardial and endocardial precursor cell populations towards the embryonic midline (A). Endocardial precursor cells begin their medial migration first, followed by the myocardial precursor cells. This medial movement is followed by the fusion of the two bilateral populations at the midline (B). Following cardiac fusion, deformation and movement of these cells gives rise to the heart tube, which all subsequent heart development builds upon (C). (D) Depicts a cross-section of the heart fields at the dashed line shown in (B). Endocardial precursor cells, having initiated the medial migration, are the medial-most cell type, encompassed by a ring of myocardial precursor cells. Both the myocardial and endocardial cells are adjacent to the endoderm, whose specific role in driving the process of cardiac fusion remains unknown. Endocardial cells (green), myocardial cells (purple), endodermal cells (yellow), outline of developing embryo (black), "s" denotes somites. Figure courtesy of Dr. Joshua Bloomekatz.

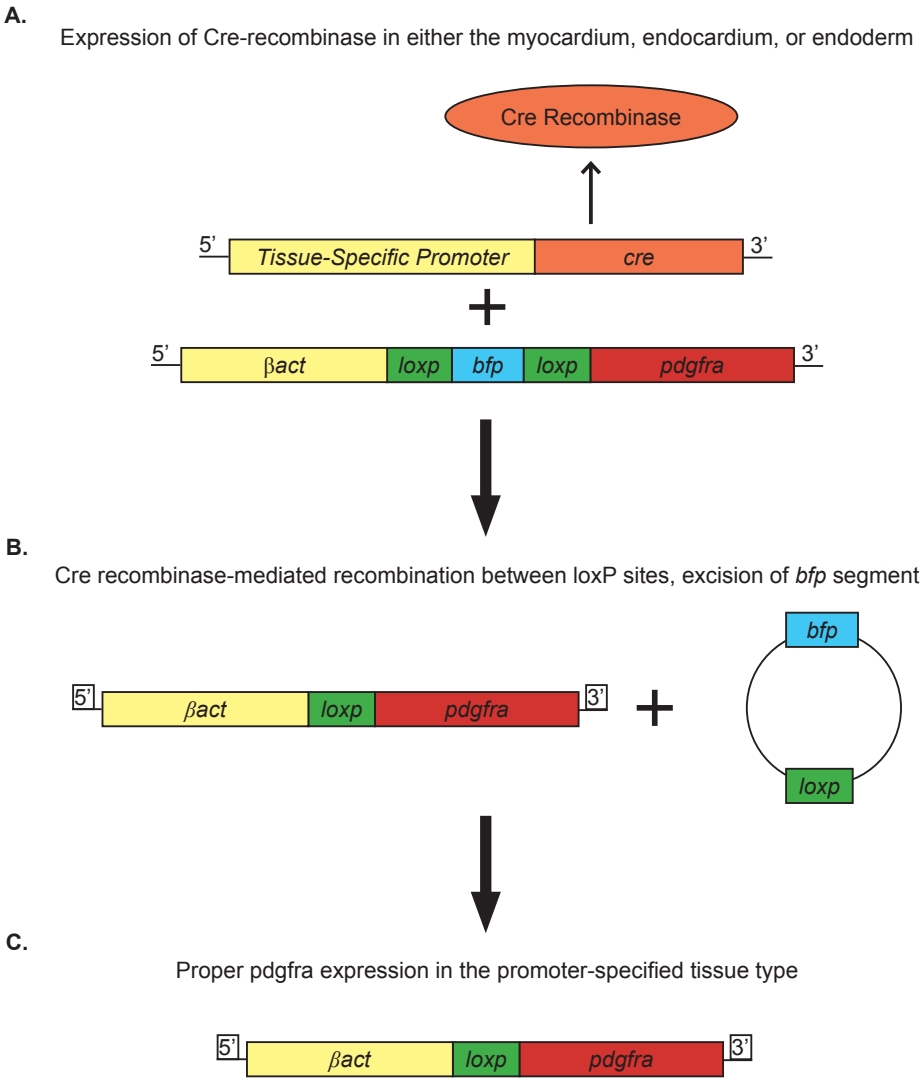

Figure 2: Cre/LoxP System Overview
(A) Tissue-specific promoters for either the myocardium, endocardium, or endoderm, ensures Cre recombinase (orange rectangle) expression is restricted to those respective tissues. The *β-actin* promoter is ubiquitously stimulated, ensuring that the *pdgfra*-containing construct is expressed throughout all tissue-types. However, the upstream gene, *bfp,* serves as a fluorescent tag and contains a stop codon at its 3' end, ensuring that in its presence, downstream elements are not be expressed. When used in concert with the ubiquitously expressed *pdgfra*-containing transgene, Cre recombinase catalyzes homologous recombination between the loxP sites (B), excising the *bfp* element and allowing for downstream expression of pdgfra (C).

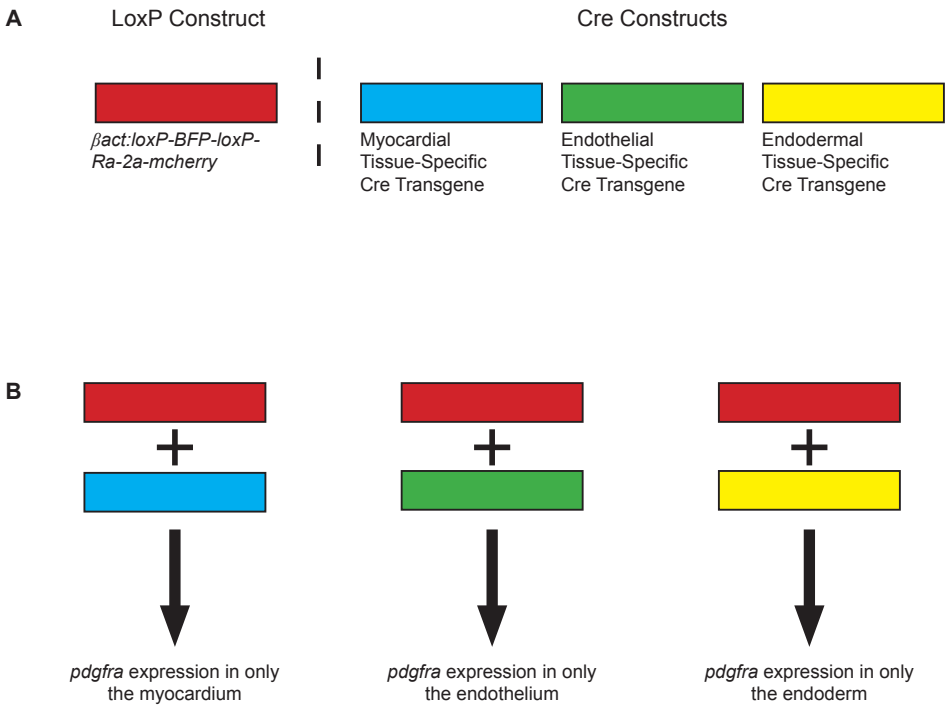

Figure 3: *pdgfra* Project Overview

(A-B) Outlines the crossing scheme enabling tissue-specific expression of *pdgfra* in either the myocardium, endocardium, or endoderm. (A) Four transgenic constructs (depicted here as rectangles) are used. One construct *Tg(βact:loxP-BFP-loxP-Ra-2a-mcherry)* carries the gene of interest, *pdgfra*, and contains loxP sites flanking a fluorescent gene, *bfp*. The presence of the *loxP-BFP-loxP* sequence will block downstream expression of *pdgfra* until Cre recombinase-mediated homologous recombination occurs between the loxP sites, due to the stop codon on the 3' end of the *bfp* gene. The remaining three constructs are Cre-containing, differentiated by their tissue-specific promoters for the myocardium (blue), endothelium (green), or endoderm (yellow). This tissue-specificity ensures Cre recombinase-mediated homologous recombination occurs only in the tissue of interest. (B) When in the presence of the loxP transgene (red), the Cre recombinase produced by each respective *cre*-containing transgene (blue, green, yellow) will result in excision between the loxP sites, removing the *bfp* gene and the tissue specific expression of *pdgfra*. B-actin (*βact*) is a ubiquitously expressed gene whose promoter is used to facilitate expression of the *loxP* transgene in all tissue types. Blue Fluorescent Protein (BFP) is a fluorescent protein, which also contains a stop codon on its 3' end. *pdgfra* is abbreviated as Ra. *2a* encodes a short polypeptide that is self-cleaving allowing for the corresponding translation *mcherry*, a fluorescent protein in order to validate proper homologous recombination.

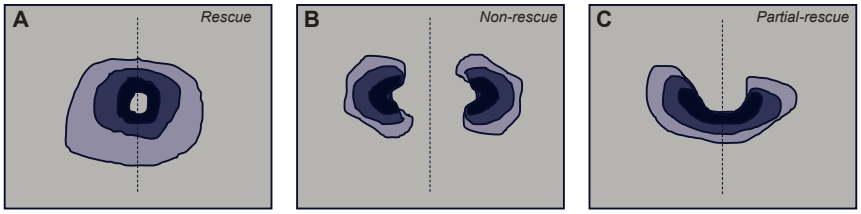

Figure 4: *in-situ* Rescue v. No Rescue

(A-C) Cartoon depictions of what will constitute a rescue after insitu hybridization to identify the location of cardiomyocytes in *ref* mutant embryos exhibiting tissue-specific expression of pdgfra. (A) A complete rescue is characterized by a single ring-shaped population of cardiomyocyte precursor cells, as is observed in wildtype embryos displaying proper cardiac fusion. No rescue (B) is characterized by incomplete ring formation, resulting in a complete lack of cardiac fusion. A partial rescue (C) will be characterized by an incomplete ring formation, characterized by a population of cardiomyocyte precursor cells that is not fully connected in a ring shape. Areas of high cell density (dark purple), areas of low cell density (light purple). Figure adapted from Bloomekatz et al. 2017.

1.1 METHODS

1.1.0: Chemical Bacterial Transformation

Chemical bacterial transformations insert a plasmid into a competent strain of bacteria in order to replicate that plasmid, creating enough amount for use in experimentation. To begin, chemically competent E. Coli, (NEB, DH10β, C3019H) are thawed on ice from –80^{oC} where they are stored. The cells are then incubated with the plasmid of interest in a microcentrifuge tube (on ice, 30 minutes) and exposed to a heat shock (45 seconds, 45 ^{oC}, using either a heat block or water bath). Following heat shock, the cell/DNA mix are incubated while shaking in an antibiotic-free liquid medium (SOC) (1.5 hours, 37 ^{oC}, 250 rpm), allowing for the expression of the antibiotic resistance gene on the plasmid of interest, thus ensuring that the cells containing the plasmid of interest are not killed immediately upon introduction to antibiotic. After this, the mix is placed on an LB agar plate with the desired antibiotic already mixed in. The presence of the pre-determined antibiotic ensures that only cells containing the plasmid of interest can grow and replicate. After being placed on the plate, the mix is spread using autoclaved glass beads. Next, the plates are incubated in a non-shaking incubator (overnight, 37 ^{oC}) to allow colony growth.

1.1.1: Liquid Culture Inoculation

Using a cell nutrient broth (liquid LB and agar) in combination with an antibiotic (the same as was present on the LB agar plate during transformation), post-transformation colonies are turned into liquid cultures in order to increase the amount of available bacteria. Ejectable pipette tips are utilized in order to pick individual colonies,

then placed into individual inoculation tubes. A tube ready for inoculation consists of 1 colony, 5mL of cell nutrient broth, and the proper amount of antibiotic which varies depending on the antibiotic used (kanamycin 50µg/mL, ampicillin 50µg/mL). These tubes are designed to be slightly loose when capped to allow for the entrance of oxygen into the tube during incubation, which is essential for E. Coli growth. Incubation proceeds overnight (37 ^{oC}, 250 rpm). Following incubation, tubes in which growth has occurred are characterized by a hazy liquid, starkly different from the yellow-clear look of LB liquid broth alone. This liquid culture can then be used to make a glycerol stock (for storage), or miniprepped (to obtain DNA for use).

1.1.2: Glycerol Stocks

Glycerol stocks are created so that a working stock of a genetic construct can be easily re-created, bypassing the need for a chemical bacterial transformation and proceeding directly to the inoculation of a liquid culture. In a microcentrifuge tube, 500 µL of liquid culture (immediately following inoculation) is mixed with 500 µL of a glycerol mixture (50% glycerol, 50% MilliQ water). This mixture is then frozen at –80^{o}C, where it can be stably stored for years. When more of the genetic construct is required, all that needs be performed is the inoculation of a liquid culture from a stab of the frozen glycerol stock.

1.1.3: Plasmid Miniprep – DNA Extraction

The goal of a miniprep is to separate the E. Coli present in the liquid culture from their plasmid DNA. Minipreps detailed in this work were performed using the Zyppy™ plasmid miniprep kit (Zymo, D4036).

1.1.4: DNA Gel Electrophoresis

DNA gel electrophoresis separates DNA samples by size by the differential speed with which different DNA sized particles move through a gel. Creation of the gel involves the mixing of powdered agarose with 1X TBE (a buffer solution containing tris base, boric acid, and EDTA), and heating until the agarose is dissolved. After a small time of cooling, a small volume (4 μL per 100 ml TBE and agarose) of ethidium bromide is added. This ethidium bromide is what allows for later visualization of the DNA bands. This is because ethidium bromide is naturally fluorescent when exposed to UV light, and fluoresces brighter when bound to DNA. Agarose polysaccharides create a gel matrix-like structure, through which the DNA moves. The movement of the DNA is facilitated by the fact that DNA is a negatively charged molecule. The DNA is loaded into the negative end of the gel electrophoresis box, so that when a voltage is applied, the molecules run to the positive end. The matrix of gel allows for easier movement of smaller molecules, which separates the DNA fragments by size (molecular weight). Following the DNA run, the gel is removed from the gel electrophoresis box and placed into a UV transilluminator. The ethidium bromide is what is visualized using this machine. Because ethidium bromide binds DNA, the DNA fragments are visualized as well. A "ladder" is added alongside the DNA fragments of interest, which consists of

DNA fragments of known sizes. This ladder is what allows for approximation of the size of the DNA fragments in the gel.

1.1.5: Multi-Site Gateway Recombination

The multi-site Gateway recombination system is a method for assembling multiple pieces of DNA together using the process of recombination. We followed the protocol from tol2kit.genetics.utah.edu and the lab of A. Untergasser. The LR reaction, which adjoins all of the desired genetic elements between the recombination sites and discard the other plasmid elements, is performed once all of the entry clones and the destination clone have been created or obtained (Figure 5). In the case of both of our transgenic Gateway constructs, three entry clones were utilized: a 5' entry clone (p5E), a middle entry clone (pME) and a 3' entry clone (p3E). The recombination sites in each plasmid, termed attachment (att) sites, are specific for other recombination sites, thus ensuring the pieces of DNA are recombined in the right order (Table 1). The attL sites match the sequence of their corresponding attR sites and no others, allowing for site-specific recombination upon addition of the proper enzyme (LR clonase II plus) during the LR recombination reaction. To begin, the DNA concentration of each clone (p5E, pME, p3E, and pDEST) was determined so that each could be diluted to the proper concentration (entry clones: 10 fmol, destination clone: 20 fmol). After obtaining the proper concentrations, the clones were mixed in a microcentrifuge tube, and the LR clonase II plus enzyme added. This mixture was then incubated overnight, followed by the addition of proteinase K, which terminates the LR reaction. Once the reaction was

stopped, the resulting Gateway DNA constructs were transformed using high competency cells.

Table 1: Att Site Sequences

attL1	CAAATAATGATTTTATTTTGACTGATAGTGACCTGTTCGTTGCAACAMATTGATGAGCAATGCTTTTTTATAATGCCAACTTTGTACAAAAAAGCAGGCT
attL2	ACCCAGCTTTCTTGTACAAAGTTGGCATTATAAGAAAGCATTGCTTATCAATTTGTTGCAACGAACAGGTCACTATCAGTCAAAATAAAATCATTATTTG
attL3	CAACTTTATTATACAAAGTTGGCATTATAAAAAAGCATTGCTTATCAATTTGTTGCAACGAACAGGTCACTATCAGTCAAAATAAAATCATTATTT
attL4	AAATAATGATTTTATTTTGACTGATAGTGACCTGTTCGTTGCAACAAATTGATAAGCAATGCTTTTTTATAATGCCAACTTTGTATAGAAAAGTTG
attR1	CAAGTTTGTACAAAAAAGTTGAACGAGAAACGTAAAATGATATAAATATCAATATATTAAATTAGATTTTGCATAAAAAACAGACTACATAATACTGTAAAACACAACATATGCAGTCACTATGAATCAACTACTTAGATGGTATTAGTGACCTGTA
attR2	TACAGGTCACTAATACCATCTAAGTAGTTGRTTCATAGTGACTGCATATGTTGTGTTTTACAGTATTATGTAGTCTGTTTTTTATGCAAAATCTAATTTAATATATTGATATTTATATCATTTTACGTTTCTCGTTCAACTTTCTTGTACAAAGTGG
attR3	CCATAGTGACTGGATATGTTGTGTTTTACAGTATTATGTAGTCTGTTTTTTATGCAAAATCTAATTTAATATATTGATATTTATATCATTTTACGTTTCTCGTTCAACTTTATTATACATAGTTG
attR4	CAACTTTGTATAGAAAAGTTGAACGAGAAACGTAAAATGATATAAATATCAATATATTAAATTAGATTTTGCATAAAAAACAGACTACATAATACTGTAAAACACAACATATCCAGTCACTATGG

1.1.6: Restriction Enzyme Cloning

The aim of restriction enzyme cloning is to utilize the 'sticky' ends created by complementary restriction enzyme digests to insert one piece of DNA (the "insert") into another piece of DNA (the "vector"). This process begins with the PCR isolation of the insert. Restriction enzyme sites are added to the ends of the of primers used for PCR so that they will be added to the insert upon PCR amplification. These restriction enzyme sites match ones present in the vector so that they create complementary overhangs. Commercially available vectors contain a multiple cloning site (MCS), consisting of multiple restriction enzyme recognition sequences in a small stretch of DNA. This MCS allows for a wide range of restriction enzyme options when deciding which to attach to one's insert. Following PCR isolation and restriction enzyme site addition, a gel purification step is performed to isolate the amplified DNA from the template DNA. Then both the insert amplicon and vector are digested with restriction enzymes. After digestions, the linearized vector is treated with a phosphatase enzyme (quick CIP) to remove the phosphates from the vector. Therefore, the phosphate used in the ligation must come from the insert DNA. This step reduces the number of false positives by ensuring that the vector does not re-ligate with itself, due to complementary ends or incomplete digestion. After CIP and another round of purification, a ligation reaction is performed using T4 DNA ligase and its associated buffer, along with the insert and vector DNA segments, at 18 C overnight.

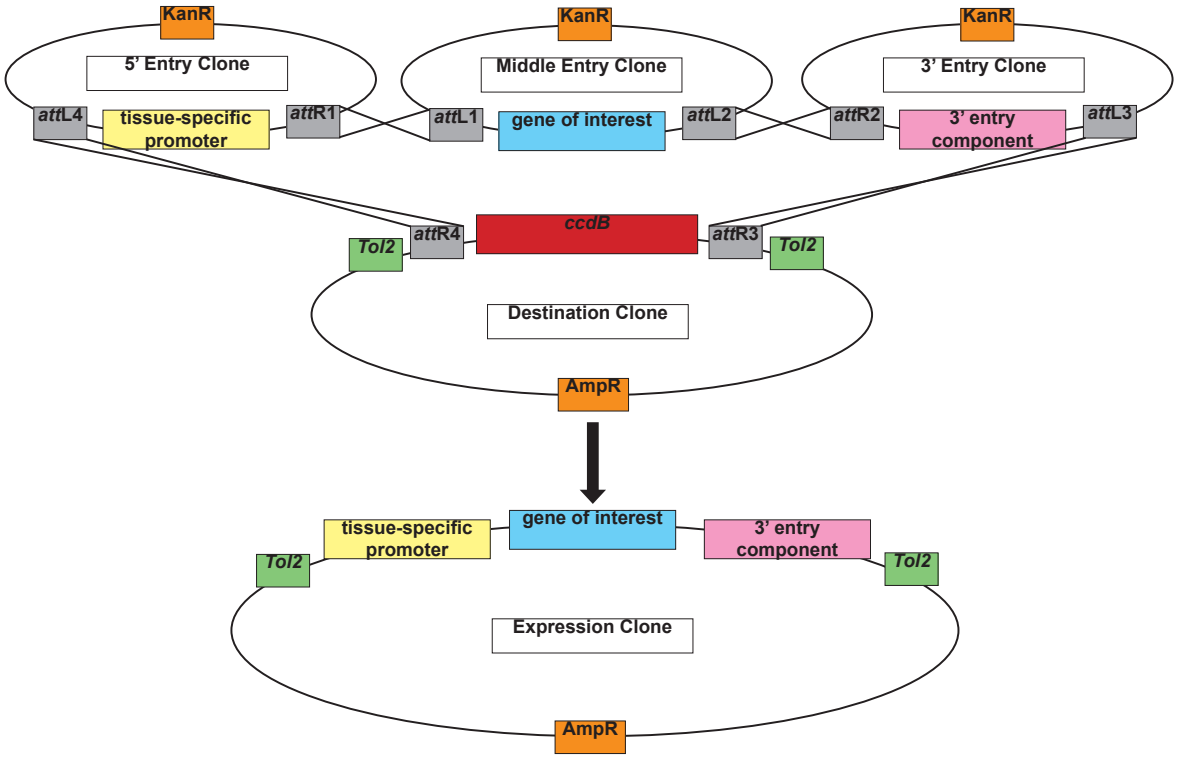

Figure 5: Gateway Multi-Site Recombination Schematic
Attachment (att) sites present on both the entry clones and the destination clone undergo homologous recombination in the presence of the proper enzyme mix, LR Clonase II Plus (a blend of integrase, integration host factor, excisionase, and reaction buffer). Att sites are genetic sites which are present in a specific organization in 5' entry clones, middle entry clones, 3' entry clones, and destination clones, that have corresponding sequences based on their numbers and letter. L sites match with R sites, and corresponding numbered sites match. The homologous recombination at these specific sites results in the formation of the final construct, the expression clone, along with the excision of the toxic ccdB gene from its position in the destination clone. The excision of the toxic ccdB gene, in combination with plating on ampicillin plates, helps to ensure that only colonies with the proper expression clone are able to grow. Antibiotic resistances (orange), promoter (yellow), att sites (gray), gene of interest (blue), 3' entry component (pink), tol2 sites (green), toxic ccdB gene (red).

1.2: RESULTS

1.2.0: *Tg(Bact:loxp-bfp-loxp-pdgfra-2a-mcherry)*

The first transgenic construct I created was *Tg(Bact:loxp-bfp-loxp-ra-2a-mcherry)* (FIGURE 6b). The function of this construct is to express *pdgfra* (denoted "Ra" above) only in tissues which express Cre, thus facilitating the tissue-specific expression of *pdgfra*. This tissue-specific, Cre-dependent expression occurs through Cre-catalyzed recombination between the loxP sites. Before recombination, the gene BFP (blue fluorescent protein), blocks the ubiquitous expression of *pdgfra*, which is downstream.

To create this transgenic construct we utilized the gateway multisite cloning system. The gateway multisite cloning system requires three unique entry vectors (p5E – 5' entry, pME – middle entry, p3E – 3' entry) and a destination vector.

The middle entry vector contains the gene of interest, in our case *pdgfra*. Although, such plasmid already exists in the lab, the *pdgfr*a gene within this plasmid contains a stop codon at its 3' end, which would block the expression of downstream elements via a P2A linker. To create a pME-*pdgfra* vector without a stop codon, we isolated *pdgfra* using a 3' cDNA preparation from zebrafish embryos at multiple embryonic stages. Following genomic cDNA isolation, primers were designed with the threefold purpose of isolating *pdgfra*, excising the stop codon, and attaching restriction enzyme sites to allow restriction enzyme cloning into a vector. Primer design was performed using previously published sequence data from Ensembl.org (https://useast.ensembl.org/Danio_rerio/Gene/Summary?g=ENSDARG00000070494;r=20:22435180-22476255). Primers were designed to amplify *pdgfra* without a stop codon, attaching SalI and NotI restriction sites on the amplicon. These restriction sites allow

pdgfra to be cloned into a pME-empty vector in the correct orientation. Following amplification of *pdgfra* including attachment of the restriction enzyme sites, a gel was run to confirm the product was the proper size. Then the band was purified via gel purification. Then the *pdgfra* amplicon and pME empty vector were digested with SalI and NotI enzymes. After these double digests, the amplicon and pME vector were purified to remove the restriction enzymes and associated buffer, and again run on a diagnostic gel (Supplementary Figure S1) to confirm single linear products and to estimate DNA concentration.

Following confirmation that the properly sized *pdgfra* insert was indeed present, a ligation reaction was performed, inserting the *pdgfra* gene (without its natural stop codon) into the empty middle entry vector. A no-insert negative control ligation was also performed. After performing the ligation reactions, a chemical bacterial transformation was performed in order to isolate fully circular plasmids containing the *pdgfra* insert. A good colony ratio between insert and no insert ligations was achieved. Multiple colonies were grown in separate liquid cultures, from which plasmids were isolated via a miniprep column kit (Zymo Research). A diagnostic restriction enzyme digest (Supplementary Figure S2) was performed on each individual miniprep in order to confirm that the insert had been properly inserted into the empty middle entry clone.

As this middle entry clone contained the gene of interest for this study, it was crucial to be certain that no mutations had occurred throughout its creation that would alter its protein expression. Due to the fact that processes like PCR can result in small mutations in the target region of DNA, which are then exponentially multiplied, it was important to take a further confirmation step than a simple diagnostic restriction enzyme

digest. Because of this, sequencing primers were designed, and in combination with our created pME:Ra sent to Eurofins Genomics in order to be sequenced. Upon receiving the sequencing results, it was found that a single nucleotide polymorphism was present in the *pdgfra* sequence of the created pME:Ra. However, because the mutation was silent (unaffecting the coded amino acid) it was decided that pME:Ra was complete, and ready for the Gateway LR reaction (Supplementary Figure S3).

The next entry clone required for the creation of the transgenic Gateway construct was the 5' entry clone, p5E:ßact:loxP-BFP-loxP. The ubiquitous nature of the *beta-actin* promoter ensures that when this construct is exposed to one of the tissue-specific Cre constructs in either the myocardium, endocardium, or endoderm, *pdgfra* and other downstream components will be expressed. The second important component of this 5' entry clone is BFP, flanked by two loxP recognition sites. BFP is terminated by a stop codon, ensuring that nothing downstream of the segment is expressed until the segment is excised through Cre-dependent recombination. Lastly, because BFP is present and expressed prior to Cre-dependent recombination, it allows for confirmation of transgene presence in the animal through fluorescent microscopy (This 5' middle entry clone was graciously sent to us from the lab of Dr. Martin Distel). The plasmid was sent to us on sterile filter paper which we soaked in water and used for chemical bacterial transformation. DNA isolated from individual colonies was used for a diagnostic restriction enzyme digest (Supplementary Figure S4) to confirm the correct plasmid.

The next required entry clone was the 3' entry clone, p3E:2a-mcherry. The inclusion of the mcherry fluorescent protein allows for confirmation of Cre-dependent recombination following the crossing of this Gateway product's line to one of the tissue-

specific Cre lines. This line was one of the original lines created for Gateway cloning in zebrafish by the Chien lab (now maintained by K. Kwan's laboratory). In order to create a working amount of the clone, a small amount was taken from a previously created glycerol stock to inoculate a liquid culture, which was then subjected to DNA isolation through a miniprep column kit. From there, a diagnostic restriction digest was performed in order to confirm that the correct clone had been isolated (Supplementary Figure S5).

The final vector required for the creation of this multisite Gateway product was the destination vector, pDESTtol2pA (acquired from K. Kwan at tol2kit.genetics.utah.edu). This destination vector was chosen firstly because it provides a polyA tail at the most 3' end of the final construct. The presence of a polyA tail aids with mRNA stability and the process of translation. It is important to note that no fluorescent protein was necessary to include in this destination vector, due to the fact that the combined use of the previously mentioned BFP and mcherry fluorescent proteins provide all of the necessary fluorescent microscopy confirmations (confirming both initial construct expression and post-Cre-dependent recombination expression).

Utilizing a previously published protocol from the lab of A. Untergasser, we performed the LR recombination reaction using pME:Ra, p5E:Bact:loxP-BFP-loxP, p3E:2a-mcherry, and pDEST:tol2pA followed by a chemical bacterial transformation. Colonies were selected from the transformation to be made into liquid cultures, which were inoculated. A miniprep DNA isolation column kit was then used, and a diagnostic restriction enzyme digest performed in order to confirm that the correct product had been obtained. The diagnostic digest returned the correctly sized result. However, it was again necessary to perform sequencing on the obtained transgenic construct, as this was the

final opportunity to confirm the product before plasmid injection into zebrafish.

1.2.1: Nkx2.5:Cre-pA

The second transgenic construct I created, *Tg(Nkx2.5:Cre-pA),* serves the purpose of expressing Cre in only myocardial cells (Figure 6a), in order to drive tissue-specific expression of *pdgfra* in the myocardium using the Tg(Bact:loxp-BFP-loxp-Ra-2a-mcherry) construct we created (see above). The Nkx2.5:Cre-pA construct was also created using the Gateway multisite recombination system.

To create the middle entry clone, pME:Cre, we began with a plasmid already present in the Bloomekatz lab, pCR8W-Cre-FRT-kan-FRT. The *cre* segment of this plasmid was amplified and isolated using PCR. Primers for PCR were designed to amplify and attach SalI and KpnI restriction enzyme sites on the 5' and 3' ends of the segment, respectively, thus allowing us to insert the *cre* amplicon into an empty middle entry clone which also contained SalI and KpnI restriction sites. Sequence data for the empty middle entry clone was obtained from tol2kit.genetics.utah.edu in order to determine the proper sites to use, and ensure that the orientation of the Cre insert would be correct upon ligation. Following confirmation that the obtained product was indeed the isolated Cre element, a gel DNA purification was performed. Then a pre-ligation restriction enzyme digest was then performed on the Cre insert and the pME-empty vector, in order to create 5' and 3' sticky ends for ligation. Both digested constructs were then put through a DNA cleaning and concentration kit, in order to ensure that a high enough concentration was present for ligation to occur. Ligation reactions were performed both with insert and without insert (negative control). Chemical bacterial

transformations of these ligation reactions showed a high ratio of colonies from the insert and vector ligation compared to the vector only ligation. DNA isolated from colonies from the transformation of the insert and vector ligation, after growth in liquid culture and miniprep, were then subjected to a diagnostic restriction enzyme digest (Supplementary Figure S6). After confirming clones which had the proper insert according to the diagnostic restriction enzyme digest, DNA from these clones were sent for sequencing to verify these clones did not contain mutations. Comparing the sequence of the clone to previously published Cre sequence data from Ensembl.com, we did not find any mutations.

For the 5' entry clone, p5E:Nkx2.5 (provided by G. Crump), the promoter sequence of Nkx2.5 was chosen due to its well-established role in myocardial cell differentiation. For the 3' entry clone, p3E:pA was chosen in order to afford the construct a poly-A tail, which provides additional mRNA stability and aids in translation. The destination vector to be used in the final Gateway product, pDEST:Tol2-cryaa-CFP [18] was chosen because it contains cyan fluorescent protein (CFP) which is expressed in the eye via the alpha-crystallin promoter. This fluorescent tag creates a transgenic mark, indicating if a particular fish contains the overall *Tg(nkx2.5:cre)* transgene.
The pDEST:Tol2-cryaa-CFP plasmid was previously created by the Bloomekatz lab.

Similar to our previous efforts in utilizing the gateway system, once having created or obtained the 5' entry (p5E-Nkx2.5promoter), middle entry (pME-cre), 3' entry (p3E-polyA) and destination (pDEST-Tol2-Cryaa:CFP) plasmids, we performed a Gateway LR reaction and chemical bacterial transformation. Individual colonies were used to inoculate liquid cultures in order to isolate plasmid DNA using a miniprep

column kit. Diagnostic restriction enzyme digests were performed on isolated plasmid DNA from 6 colonies. in order to confirm that the proper recombination product had been obtained. However, we did not identify a correct clone in these colonies. To screen through more colonies, we performed colony PCR, eventually identifying a colony that had integrated all three plasmids into the destination vector.

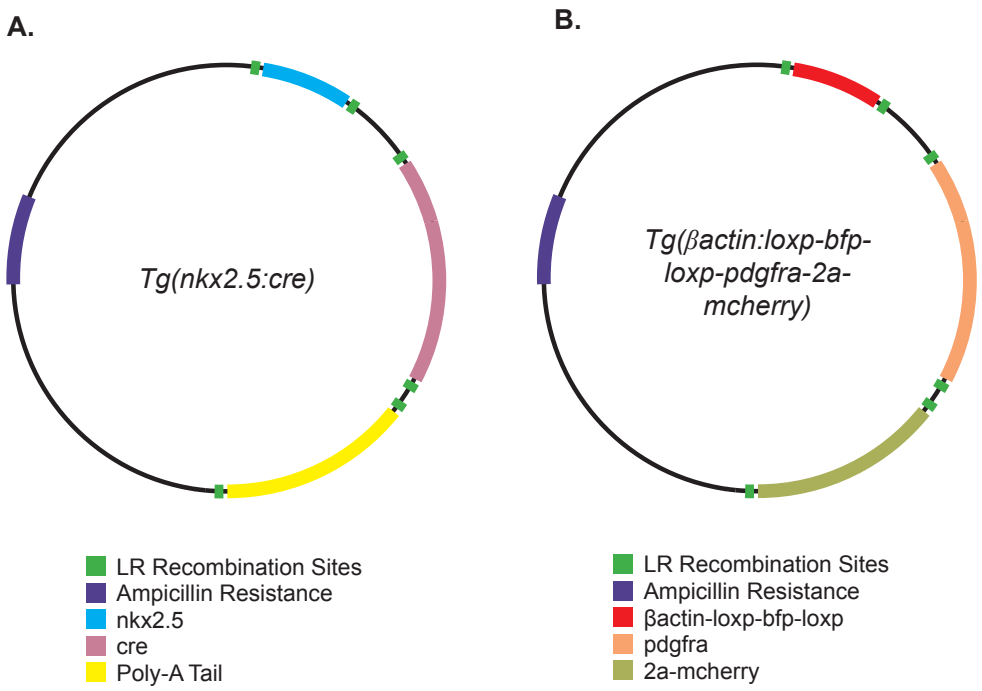

Figure 6: Gateway Expression Clones - Theoretical Maps
Theoretical plasmid maps of nkx2.5:Cre-polyA (A) and βactin:loxP-mcherry-loxP-pdgfra-2a-mCherry (B).

1.3: DISCUSSION

Through utilization of restriction enzyme cloning and the Gateway recombination system, two transgenic constructs were created for use in our project identifying the functional location of *pdgfra* during cardiac fusion. These transgenic constructs, *Tg(ßact:loxp-BFP-loxp-Ra-2a-mcherry)* and *Tg(Nkx2.5:Cre-pA)*, have now been injected into zebrafish embryos at the one-cell stage in combination with transposase RNA, to begin the process of creating lines of transgenic zebrafish. Once a stable transgenic line is isolated for each transgene, the reporter line (Bact:loxp-BFP-loxp-Ra-2a-mcherry) will be crossed with each of the three driver lines containing transgenes for tissue-specific expression of cre in the myocardium (Nkx2.5:Cre-pA), endocardium, or endoderm. These crosses will be performed using *ref* mutant zebrafish, who normally exhibit an organism-wide lack of *pdgfra* expression, thus the only *pdgfra* expression in these embryos will be due to the tissue-specific transgenics. These transgene-containing *ref* mutant embryos will, as previously stated, be analyzed using *insitu* hybridization in order to determine whether tissue-specific expression of *pdgfra* in the myocardium, endocardium, or endoderm results in a rescue of the *ref* mutant phenotype.

Upon performing *insitu* hybridization, we will be able to compare the results to our hypothesis that *pdgfra* functions within cardiomyocyte precursors in order to regulate cardiac fusion. There are multiple possible outcomes, each of which will lead to a different trajectory of future studies. Firstly, we could, in keeping with our hypothesis, find that *pdgfra* functions within myocardial precursor cells during cardiac fusion, signifying a paracrine model of signaling from the endoderm to the myocardium. If this is

found to be the case, future studies would be directed towards finding how the tissue-specific nature of *pdgfra* is achieved. Alternatively, we could find that *pdgfra* functions within the endoderm during cardiac fusion, signifying an autocrine model of signaling. In this scenario, future studies would be directed towards confirming these results through endoderm transplantation studies. Lastly, it could be found that none of the transgene-containing *ref* mutant embryos exhibit a rescue of the *ref* phenotype, indicating that *pdgfra* acts in another tissue altogether during cardiac fusion. One possible alternative cell type that *pdgfra* could work within is neural crest cells, in which case future studies would be aimed towards obtaining or creating a neural crest-specific Cre line, and performing an experiment similar to the one detailed in this study. It is, however, unlikely that *pdgfra* functions within neural crest cells due to the fact that previous studies have shown that neural crest cells are not involved in the early formative processes of the heart (Richarte et. al 2007, Tallquist & Soriano 2002).

A future study examining the functional location of pdgf-aa, a Pdgfra ligand, would also complement the results of this study. Although previous studies (Bloomekatz et. al 2017) have indicated that *pdgfaa* functions within the endoderm, a study similar to this one, in which *pdgfaa* is expressed in a tissue-specific manner in either the myocardium, endocardium, or endoderm, would serve to further support this claim. Validating the functional location of *pdgfaa* would allow a better understanding of the PDGF signaling system during cardiac fusion.

Altogether, the transgenic constructs created through this work will lead to a deeper knowledge of the molecular mechanisms employed during PDGF signaling. This has the possibility of not only driving future studies of PDGF signaling, but the process

of heart formation as a whole. Due to the fact that multiple cardiac diseases are caused by an irregularity during cardiac morphogenesis, and cardiac fusion is the first step in this complex process, this research has the potential to reveal new information regarding the causes and proper treatments of CHDs.

II: Aid in the Creation of a Review Chapter: Zebrafish as a Model for Congenital Heart Defects (CHDs)

2.0: INTRODUCTION

Congenital heart defects are a broad class of defects, grouped because of their key similarity: an effect on the structure and functionality of the individual's heart. In the United States today, approximately one in every one-hundred live births is affected by a CHD. With a rate of incidence this high, CHDs are the most common form of birth defect in the United States [1]. Among individuals born with heart defects, one in four will require surgery within the first year of life [2]. The combined prevalence and often severe nature of CHDs make them a major health issue facing the United States.

Because of the incidence and severity of CHDs, they have been the topic of study for many researchers utilizing zebrafish as a model organism. Zebrafish were elected as the model organism for this study for multiple reasons. As is important in any model organism, the zebrafish genome displays a high level of molecular conservation with humans, meaning that studies performed in zebrafish can be translated to the associated human process or disease [30]. In particular, the process of cardiac development and cardiac morphology are similar between humans and zebrafish. Additionally, zebrafish offer many advantages compared to mice as a model organism. They are small and numerous, meaning large numbers can be stored in a single aquatic facility. This, coupled with a lower cost of maintenance, makes zebrafish a cost-effective model [31]. Also, because zebrafish fertilize externally, embryos are much easier to access for genetic techniques, such as plasmid injection at the one-cell stage. Additionally, the embryo is transparent meaning that developmental processes can be observed using only a

microscope, without the need for parent dissection or interruption of development [32] as is required with mice. In addition to these benefits, zebrafish are excellent candidates for studies in heart formation, due to the similarities they share with humans.

Although zebrafish possess a two-chambered heart, the general structure is quite similar to a human. Both have a closed cardiovascular system driven by a central pumping organ. Additionally, the cardiac chambers of both human and zebrafish consist of an inner layer of endocardial cells covered in a layer of muscular myocardial tissue [33]. Physiologically, zebrafish and humans are also similar. Both exhibit similar spontaneous beating rates, and a cardiac action potential which is characterized by a long plateau phase. Lastly, the contractions of both species' hearts are regulated by conserved ion channels within cardiomyocytes and specialized cells, such as pacemaker cells. [34, 35]

Studies modeling CHDs in zebrafish serve a crucial role, in that they help to identify the cellular and molecular mechanisms that guide the formative processes of the heart. This means that their results shed light on the causes of what goes wrong in the genesis of CHDs. In addition to my work in identifying the functional location of *pdgfra*, I also aided my research advisor, Dr. Joshua Bloomekatz, in drafting a chapter reviewing the use of zebrafish in studying the molecular basis of congenital heart defects. This review chapter examined the tools that zebrafish researchers used to examine and model CHDs, as well as the findings of their associated studies. My work on this project mainly consisted of creating multiple figures for use in the chapter. Additionally, part of my work in this endeavor involved reviewing, fact-checking, and spell-checking the chapter as it neared completion.

2.1: RESULTS

2.1.0: Sarcomere/Cardiomyocyte Figure

The vital function of the heart, contraction, occurs due to the interaction between actin and myosin filaments. However, in order to fully comprehend this seemingly simple interaction one must understand the cellular and subcellular structures involved in the contraction of the heart. The troponin-tropomyosin complex (consisting of troponin I, troponin C, troponin T2, and tropomyosin) attached to actin filament undergoes calcium dependent changes which result in the contraction or relaxation of sarcomeres through the binding, pulling, and releasing of myosin to actin. At their ends, myosin and actin filaments are bound to Z-discs, which serve as connection points between sarcomeres. Attached to these Z-discs is titin, a large protein complex which stretches the length of the sarcomere and binds myosin, in order to anchor it to the Z disc.

Multiple CHDs have been found to involve a disruption of sarcomeric genes. Previous studies have shown that a mutation of the titin gene (*ttn*) in zebrafish, called *pickwick* (*pik*), results in the development of a heart displaying a dilated cardiomyopathy (DCM) phenotype. Human patients with a mutation in *ttn* display similar DCM phenotypes. Additionally, a mutation in the zebrafish troponin T type 2a (*tnnt2a*) gene called *silent-heart* (*sih*) results in embryos with a variety of phenotypes, including a non-contractile heart, pericardial edema, and sparse sarcomere formation. Lastly, mutations in the myosin gene have also been studied for their implication in the development of CHDs. For example, zebrafish studies have shown that mutations in *myosin heavy chain 6* (*myh6*) and *myosin heavy chain 7* (*myh7*) resulted in the

development of hypertrophic cardiomyopathy (HCM) and DCM phenotypes. Humans with mutations in *myh6* and *myh7* display similar phenotypes.

In order to show the complex interplay between all of these components, I created a figure depicting a cardiomyocyte at the cellular level, along with an in-depth view of the subcellular components of the sarcomere. Additionally, the figure displayed the sarcomeric dynamics in the absence, and presence of calcium. Only through understanding the components involved in the contraction of the heart is it possible to study the effects of their errant expression. This figure (Figure 7) served the purpose of providing readers with a visual reference for the multiple interconnected structures involved in the dynamic interplay between two cardiomyocytes, which were discussed at length in the review in reference to their ability to be causal agents of congenital heart defects when improperly expressed.

2.1.1: TTNtv Figure

In recent studies researchers have observed and researched the intriguing phenomenon, that patients exhibiting DCM are more likely to have truncating mutations in *ttn*, titin truncating variants (TTNtvs) at the C-terminus (C-term) of a gene rather than the N-terminus. N-terminal (N-term) truncations tend to be less severe. This is intriguing due to the fact that a mutation of the N-term (early) should be expected to result in a severely truncated protein, and therefore a more severe phenotype than a C-terminal (late) truncation. Multiple hypotheses arose as possible answers to this problem. One such hypothesis proposed that C-term TTNtvs could result in the formation of a dominant-negative mutation. In order to study this hypothesis, researchers went about

creating zebrafish models for C-term and N-term TTNtvs. One such study utilized a CRISPR/Cas9 and TALEN based approach in order to introduce stop codons (truncating agents) in either the N or C-terminus of *ttn* [11]. This study set out to investigate the hypothesis that C-terminal truncations could possibly be creating a dominant-negative mutation by creating a double mutation in zebrafish, with both an N and C-term TTNtv. These double mutant fish displayed phenotypic similarities to the C-term mutants, suggesting that a dominant-negative behavior is unlikely for C-term mutations.

Another hypothesis tested through zebrafish models proposed that C-term TTNtvs are simply in exons with higher usage. This hypothesis was generated through preliminary studies finding a significant correlation between exon usage and TTNtv pathogenicity. Through this study it was discovered that zebrafish TTNtv's in exons known to have high usage rates display more severe phenotypes, which provided support for this hypothesis. Ultimately, more studies are required before an explanation for this unique finding can be generated.

In order to display this interesting finding, and the zebrafish studies performed to recapitulate and study the dominant-negative hypothesis, I created a figure displaying real examples of human and zebrafish TTNtvs. This figure (Figure 8) depicts both N-term (early) and C-term (late) mutations of the titin gene in both humans and zebrafish.

2.1.2: Human v. Zebrafish AP / Zebrafish ECG Figure

The reason that studies like that involving the C-term TTNtvs can be studied in zebrafish and analyzed alongside human data owes to the striking similarity between zebrafish and human cardiac structure and electrophysiology. Similarities in

electrophysiology also allow zebrafish researchers to conduct studies regarding cardiac conduction defects that can be analyzed in comparison to humans.

In order to display this striking similarity, I created a figure (Figure 9) depicting a human ventricular action potential (AP) as compared to that of a zebrafish, as well as a typical zebrafish electrocardiogram (ECG). In both zebrafish and humans, APs begin from rest with a rapid depolarization phase and are followed by a slow repolarizing phase and finally a rapid repolarizing phase. The only notable difference between the two species is that zebrafish lack a distinct early repolarization phase following initial rapid depolarization, as is observed in humans. In addition to the similarity in ventricular action potential shape, this figure also served to show the shape of a typical zebrafish electrocardiogram (ECG or EKG). As with the action potential, the key components of the zebrafish ECG resemble very closely those of a human. The coupling of these two facts provide an easy-to-grasp benefit of using zebrafish as models to study human electrophysiological defects.

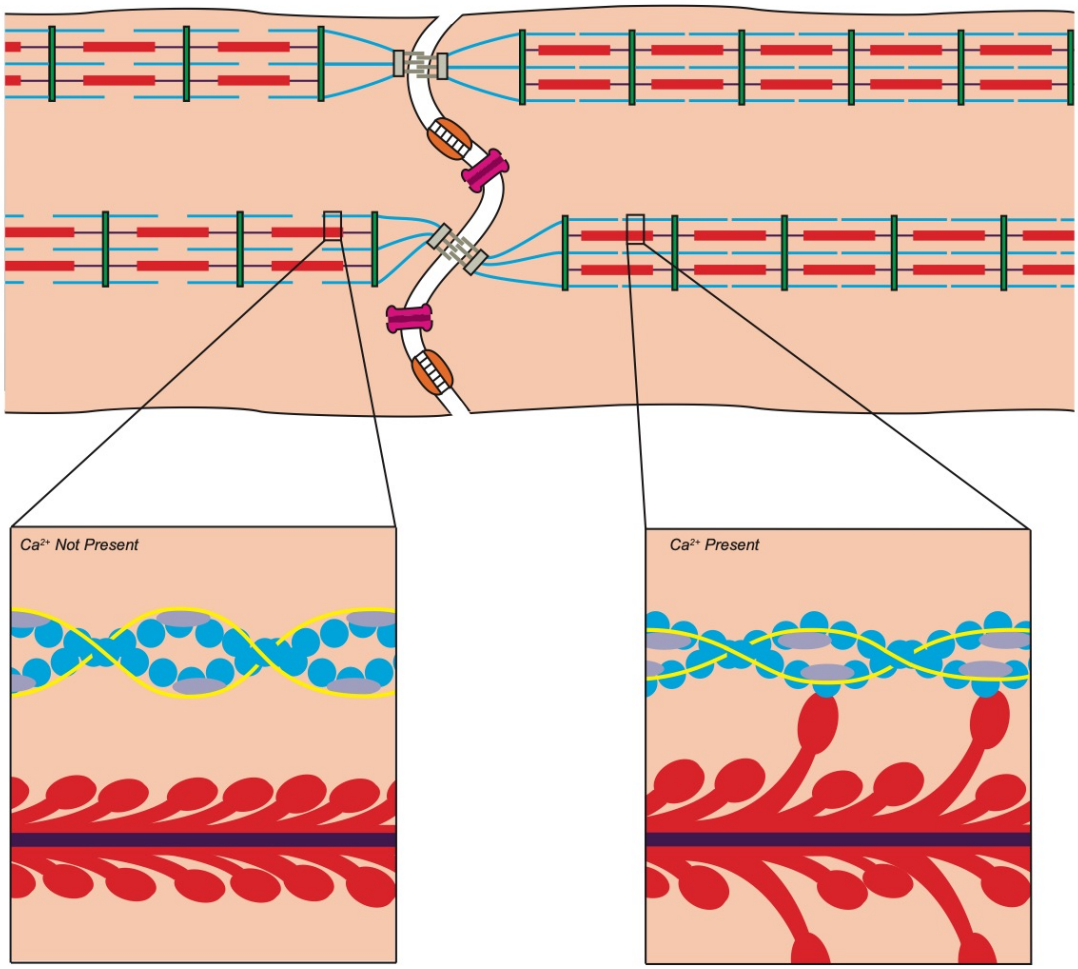

Figure 7: Cartoon of adjoined Cardiomyocytes and Sarcomere Dynamics
In the absence of Ca^{2+} (left cell and inset) the myosin filament (red) is not bound to the actin filament (blue), and no contraction occurs. In the presence of Ca^{2+} (right cell and inset), Ca^{2+} ions bind troponin C (light purple) which pulls tropomyosin (yellow) away from the myosin-binding sites present on actin filaments. With binding sites available, the myosin filament binds the actin filament, resulting in cell contraction. Both the myosin and actin filaments are bound on their ends to the Z-disc (green). Titin (dark purple) extends from one Z-disc through the middle of the myosin filament, meeting and binding the end of another titin molecule at the halfway point (the M-line) of the sarcomere. Titin anchors the myosin filament at the Z-disc. Figure adapted from Bers et al. 2019, Harvey et al. 2011, Al-Khayat et al. 2013, Estigoy et al. 2009.

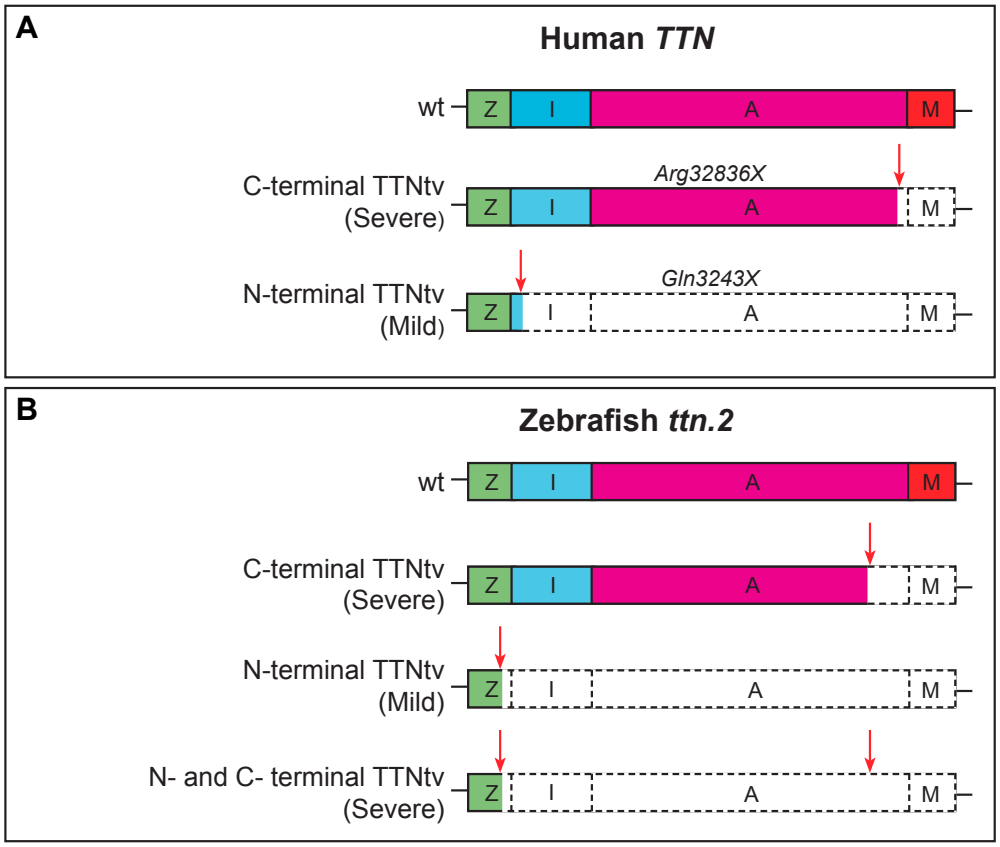

Figure 8: Location of Human Titin Truncating Variants (TTNtvs) and Associated Zebrafish Studies (A) Titin truncating variant (TTNtv) mutations (mutations in resulting in an early truncation of the translated protein) in human patients with dilated cardiomyopathy (DCM) are more often found in the C-terminus of the protein. TTNtv in the N-terminus are often mild or silent. Representative examples are shown: A TTNtv (Arg32836X) from a patient with end-stage DCM and a TTNtv (Gln3243X) from a healthy individual. (B) Gene editing was utilized to model C-terminal and N-terminal human truncations in zebrafish. Also, a mutant was created possessing both N-term and C-term truncations. These double mutants display C-terminal truncation phenotypes suggesting that a dominant-negative mutation, as hypothesized by Zhou et al., is not made in C-terminal truncations. Arrows (red) indicate location of the truncation. Figure adapted from Herman et al. 2012, Roberts et al. 2015, Schafer et al. 2017, Shih et al. 2016.

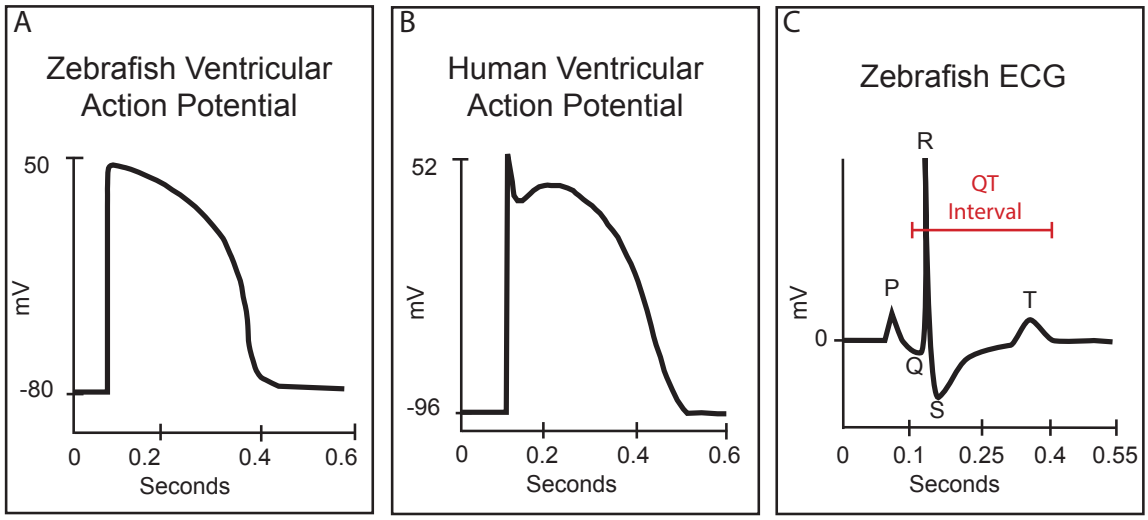

Figure 9: Zebrafish and Human Ventricular Action Potential (AP) and Zebrafish Electrocardiogram (ECG)

Representative zebrafish and human ventricular action potentials (AP) are depicted (A, B). The zebrafish ventricular action potential (A) is similar to the human ventricular action potential (B), although it lacks the initial, rapid repolarization that is observed in the human ventricular action potential. Also depicted is a typical zebrafish electrocardiogram (ECG) (C) which is also similar to a human ECG (not shown), including its distinct P, Q, R, S, and T phases, along with the QT interval. Figure adapted from Liu et al. 2016, Poon et al. 2013.

2.2: DISCUSSION

In summation, my work in the creation of multiple figures, fact-checking, and revising helped lead to the completion of a review chapter which will serve as a reference of the tools that zebrafish researchers have used, and are currently using to study the genesis of CHDs. The first of these highlights the structure of a cardiomyocyte, with an added emphasis on sarcomere dynamics and the process of contraction at the sarcomeric level. This figure will help to provide readers with a reference point for future discussions regarding the errant function of the components involved. Additionally, I was able to depict the interesting finding regarding one gene, *titin (ttn*). TTNtvs (TTN truncating variants) display a more severe phenotype when present on the C-terminus of a protein compared to the N-terminus. An important part of this figure was that, while originally characterized in humans, zebrafish models have been instrumental in deciphering and testing different possible causes. I also sought to create a figure that was accessible to readers unfamiliar with genetic mutations or even the difference between the C and N-terms of a polypeptide. The third and final figure depicts a human ventricular action potential alongside a zebrafish ventricular action potential, along with a typical zebrafish ECG. Through a side-by-side comparison of these electrophysiological factors, this figure serves to highlight the striking electrophysiological similarities between zebrafish and humans.

My work creating these figures, reviewing, and fact-checking for the review chapter, written by the Bloomekatz group, helped lead to the completion of the project as a whole. At this point in time, the chapter has been accepted and is pending publication [Shrestha, R., Lieberth, J., Tillman, S., Natalizio, J., Bloomekatz, J. (2020) “Using

Zebrafish to Analyze the Genetic and Environmental Etiologies of Congenital Heart Defects" in Animal Models of Human Birth Defects, Springer Nature, Singapore].

Upon publication, the review chapter as a whole and the figures to which I contributed will hopefully be read and seen by professors, researchers, medical professionals, and students. Specifically, I hope the figures that I created will serve as visual guides for topics, involving the complexities and advantages of using zebrafish as a model organism to study early heart defects, cardiac electrophysiology, TTNtv's, cardiomyocyte structure and function, and the molecular basis for contraction of cardiac cells.

III: 3D Printing Project

3.0: INTRODUCTION

The recent increases in accessibility and affordability of 3D printers now allows for the construction of specialized equipment by individual labs, which previously either had to be purchased from specialized manufacturing companies at highly marked up prices or was unavailable. In particular, the availability of 3D printers in the IDEA laboratory in the University of Mississippi (UM) library and the Center for Manufacturing Excellence's (CME) makerspace at UM has allowed us to construct several pieces of equipment. In addition to other work performed in the Bloomekatz Lab, I was tasked with modeling and printing three pieces of equipment for the lab: confocal microscope slide holders, a zebrafish feeding gun apparatus, and a gel electrophoresis comb.

Each project arose from a different combination of functionality and cost. For example, the Bloomekatz Lab possessed confocal microscope slide holders prior to my joining. However, they were significantly costly, especially considering their simplistic design and lack of necessity for being a specific material. On the other hand, the zebrafish feeding gun apparatus was something which had never been used in the Bloomekatz Lab, nor anything like it. Instead, a scoop system was in use which often left tanks being unevenly fed, and notably dirty. The initial desire for the creation of this piece of equipment was then out of functionality, to fill a need in the lab through a piece of equipment which would improve quality and speed of work. There are feeding apparatuses available for sale online, however they are also quite expensive. Lastly, the

gel electrophoresis comb project was pursued due to the relatively high cost of this piece of equipment, and the ready availability of models.

3.1: RESULTS & DISCUSSION

The first 3D printing project I undertook was creating confocal microscope slide holders. In confocal microscopy, samples can be mounted onto glass coverslips in order to be visualized. In turn, the glass coverslips are placed onto a slide holder. These items are traditionally expensive or even unavailable, even though they have a relatively simple geometry, and the material which they are made from is not important for their function as a microscope slide holder. Through a simple model and the help of the University of Mississippi's IDEAlab, I was able to create microscope slide holders printable for less than a dollar each. The model was designed using Fusion360, free modeling software available from Autodesk, and printed using a Lulzbot TAZ 6 3D printer. Polyactic acid (PLA) was chosen as a material. Printing was performed using a low infill (5%), due to the fact that the slide holder is small and needs to be flat and smooth in order to properly hold a microscope slide. Because microscopy is a crucial element in almost all projects in the Bloomekatz lab, these slide holders will benefit lab members at a low cost for years to come.

The second 3D printing project I undertook was the creation of a feeding gun. Maintenance and upkeep of an aquaculture facility can be incredibly time-consuming and take away from time spent in the lab. Normally, food is dispensed using a set of feeding scoops of various sizes. This system is laborious and time-consuming, because feeders must use three different scoops (a plastic pipette for babies, a "nip" for adolescents, and a "smidgen" for adults) and three different food sizes (Gemma micro 75 for babies, Gemma micro 150 for adolescents, Gemma micro 300 for adults) (Available from Skretting USA). Feeding apparatuses, which speed up the process, are available for

purchase from certain companies, but are quite costly. For these reasons, I worked on creating a 3D-printed feeding gun apparatus, in order to cut down on the time spent during facility-wide feedings, while still delivering the proper amount of food to each tank. A model was already available from Marc Tye, from the University of Minnesota Twin Cities. This model consists of six individually printed parts: a bottom, handle, lever, pivot, slider, and top. Again, the University of Mississippi's IDEA lab's TAZ 6 printer was used. The parts were printed using PLA at a standard infill of 25%, in order to provide a balance between durability and smoothness. All 6 parts have been assembled, and the device has been shown to fit a microcentrifuge tube (which is connected to the top of the apparatus as to hold the food). However, more customization and optimization are needed to make this apparatus functional. This customization includes redesigning the dispenser and/or the trigger mechanism to ensure that a consistent amount of food is delivered with each pull. Additionally, this will include testing whether the amount of food present in the gun's food storage compartment alters the amount dispensed. Also, the overall cleanliness of the tanks following use of the gun, and if the gun is prone to food jams, needs to be assessed. Each of these obstacles defeat its intended purpose as a time-saving piece of equipment.

Lastly, I have begun research and work on creating gel combs, for use in DNA gel electrophoresis. Similar to these other projects, the cost of purchasing the item from a company seemed more expensive than was necessary. Through models available online at yeggi.com, a model (https://www.thingiverse.com/thing:352873/files) was selected and test printed. However, due to the fact that the gel comb would need to have very smooth teeth, in order to ensure the proper running of DNA from the wells it created, a higher

quality 3D printer was required. A higher-quality stereolithographic printer from the makerspace in the Center for Manufacturing Excellence was used for this reason. While the 3D printed gel comb produced had the proper dimensions, it was prone to chipping and breaking off of the teeth, meaning that future work towards creating a functional product will need to involve optimizing the comb's dimensions, as well as the material used to create it.

All of the models which I worked on during my time in the lab and notes on their creation have been saved, and will be available for future members of the lab to access. Through this, the models can be continuously reprinted in the case that more of the designed objects are required. Additionally, this ensures that should a future lab member wish to continue work on either the feeding gun apparatus or the gel electrophoresis comb, they will have all of the resources necessary to do so.

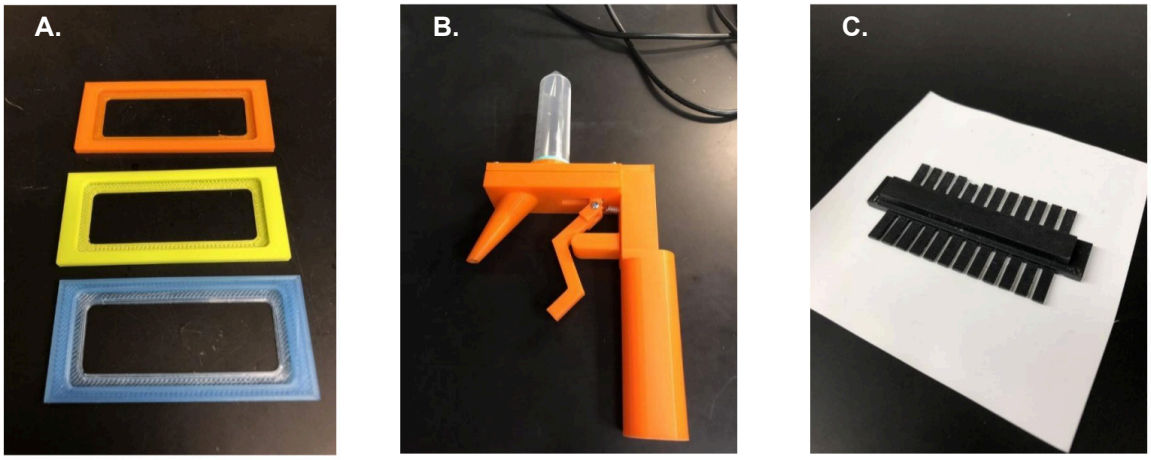

Figure 10: 3D Printing Projects
Depicted are 3D printed confocal microscope slide holders (A), feeding gun apparatus (B), and gel electrophoresis comb (C). (A) was designed from scratch using Fusion 360, and printed at the University of Mississippi's IDEA lab. (B) was created from a design provided by Marc Tye, from the University of Minnesota Twin Cities, edited and scaled using Fusion 360, and printed at the University of Mississippi's IDEA lab. (C) was created based on a previous design discovered on the 3D model sharing site thingiverse.com (https://www.thingiverse.com/thing:352873/files), edited and scaled using Fusion 360, and printed at the University of Mississippi's Center for Manufacturing Excellence's maker-space.

IV: Supplemental Materials

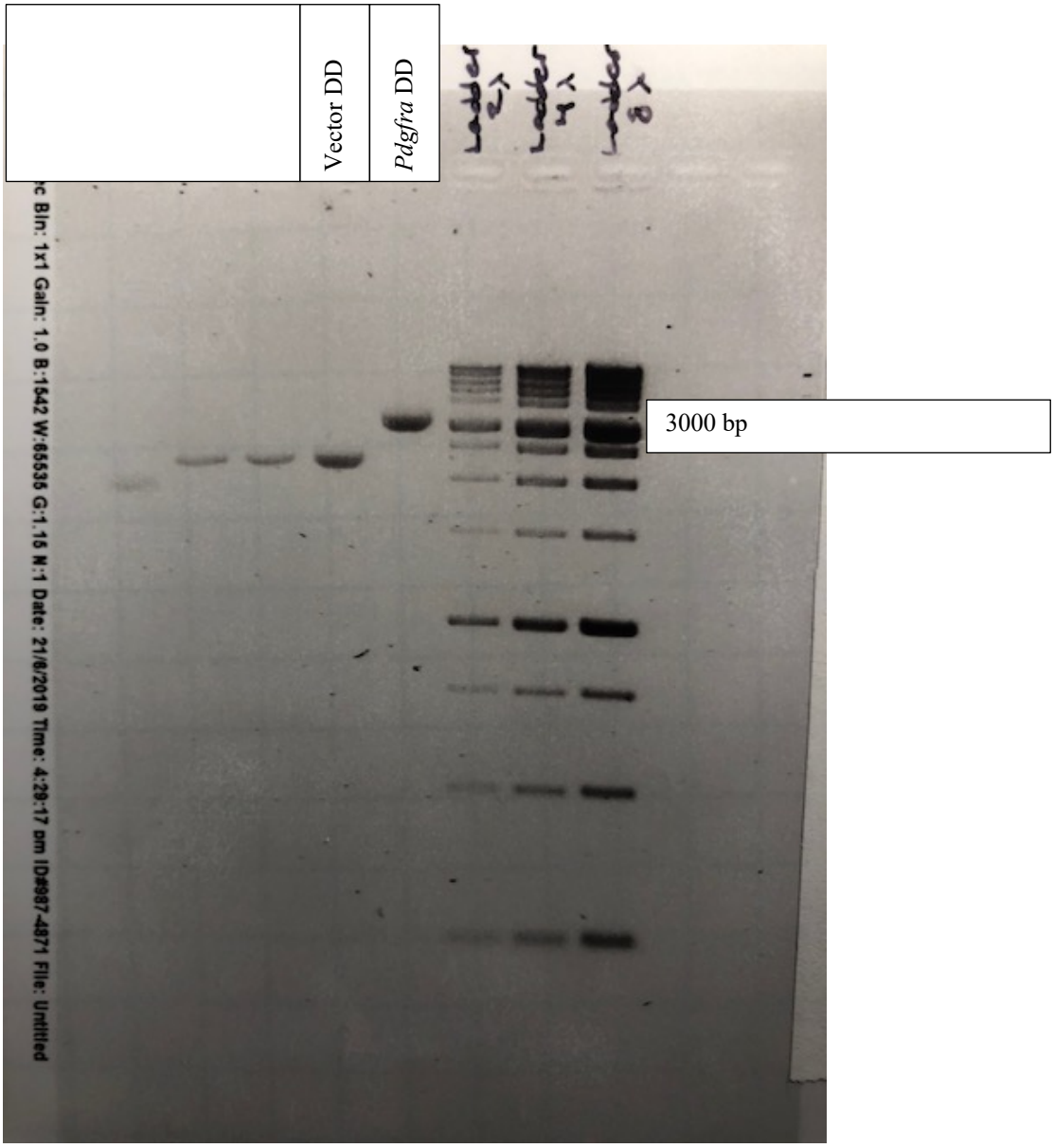

Figure S1: Gel digest – Pre-digest Ligation of *pdgfra* and empty middle entry clone
The *pdgfra* insert and empty middle entry clone were both double digested prior to their ligation. This gel was ran to confirm the size of both of these prior to the ligation reaction.

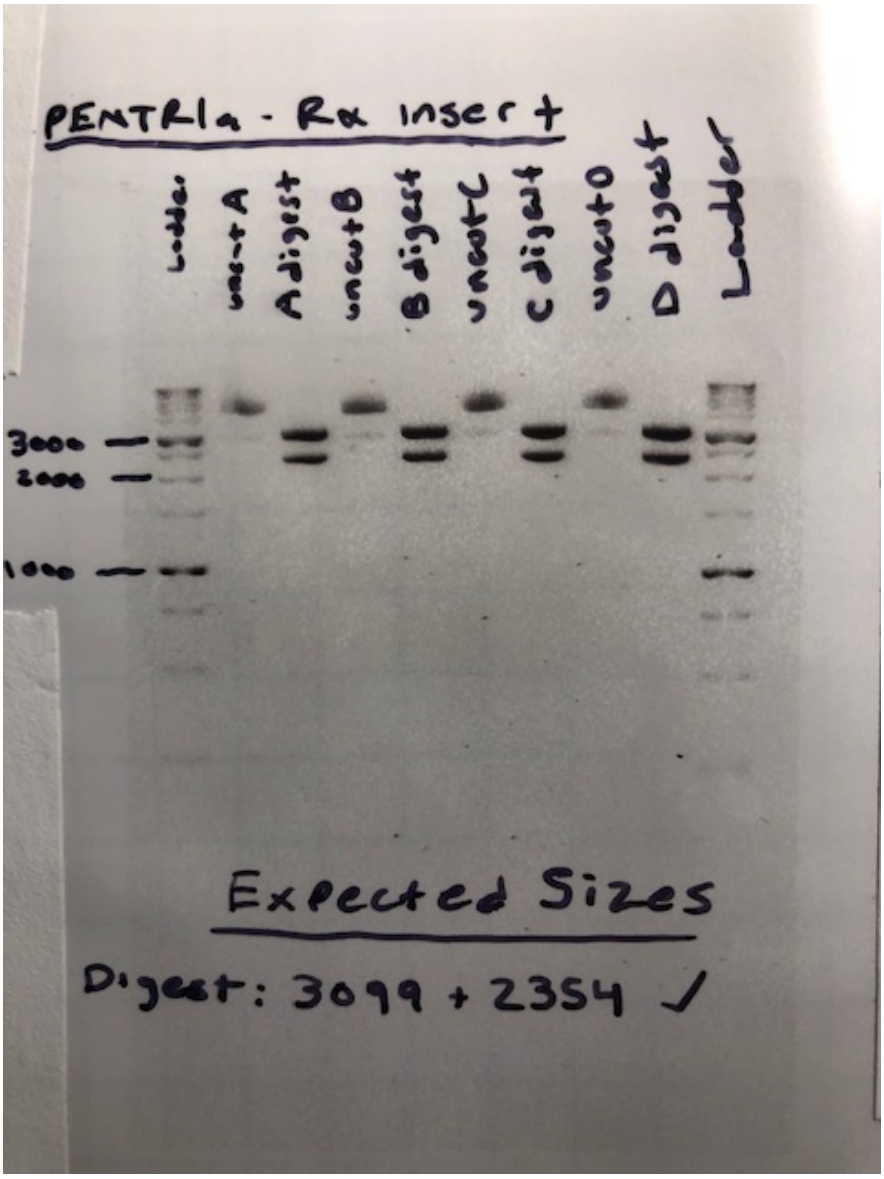

Figure S2: Gel Digest – *pdgfra* Ligation
Following the ligation of *pdgfra* into the empty middle entry clone, this gel was ran in order to confirm proper ligation. Expected product sizes of digested ligation: 3099 bp, 2354 bp.

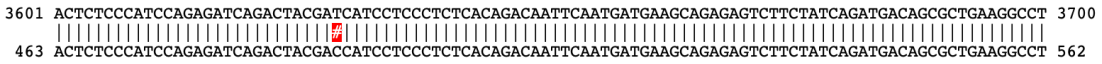

Figure S3: Sequencing – *pdgfra* Ligation into Empty Middle Entry Clone
Following the ligation of *pdgfra* into the empty middle entry clone, the ligation product was sequenced in order to confirm both that the two had been ligated properly and that there were no mutations present. The top sequence represents a wildtype *pdgfra* gene sequence, while the bottom sequence represents a sequence selection from the sequenced ligation product. Seen as a red line, there is a mutation present in the ligation product at the 491th base pair. This mutation proves to be silent though. The wildtype codon, ACT, codes for the same amino acid (threonine) as the mutated form, ACC.

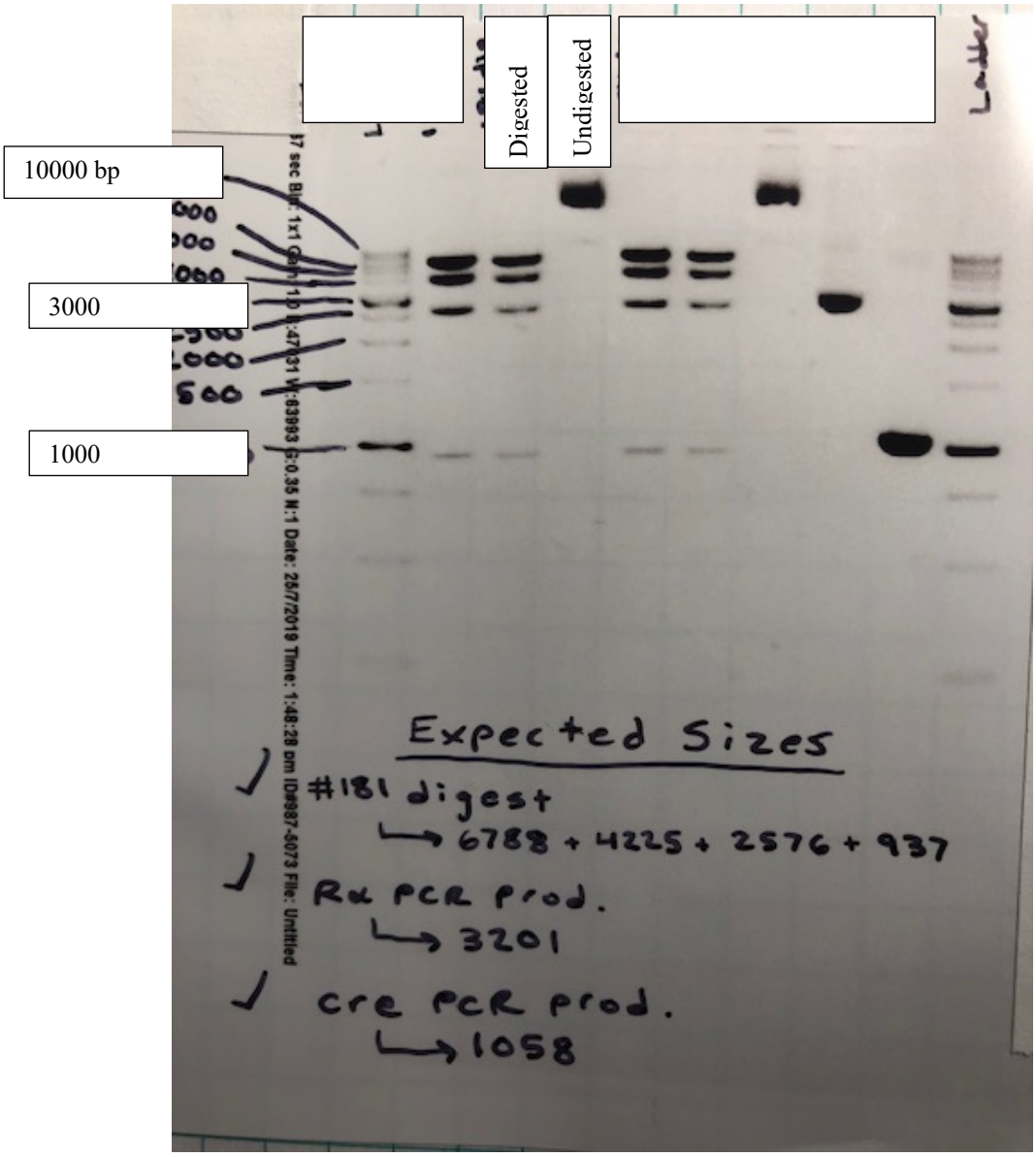

Figure S4: Gel Digest: p5E:ßact:loxP-BFP-loxP
Following transformation of p5E:ßact:loxP-BFP-loxP, a gel digest was ran in order to confirm that the received plasmid was the correct one. Expected digested cut sizes: 6788 bp, 4225 bp, 2576 bp, 937 bp.

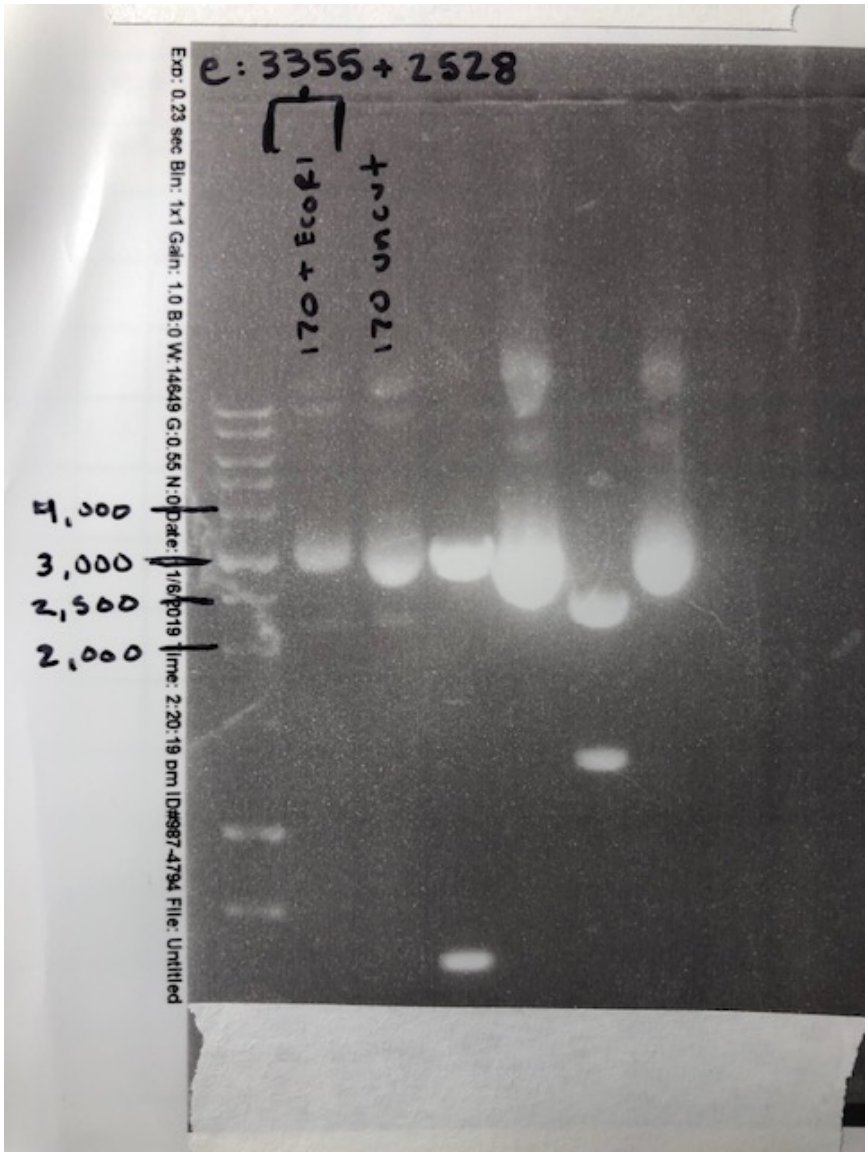

Figure S5: p3E:2a-mcherry
Following transformation of p3E:2a-mcherry from the available stock, this digest was ran in order to confirm the correct plasmid was indeed present. Expected digested product sizes: 3355 bp, 2528 bp. "170"denotes the plasmid p3E:2a-mcherry.

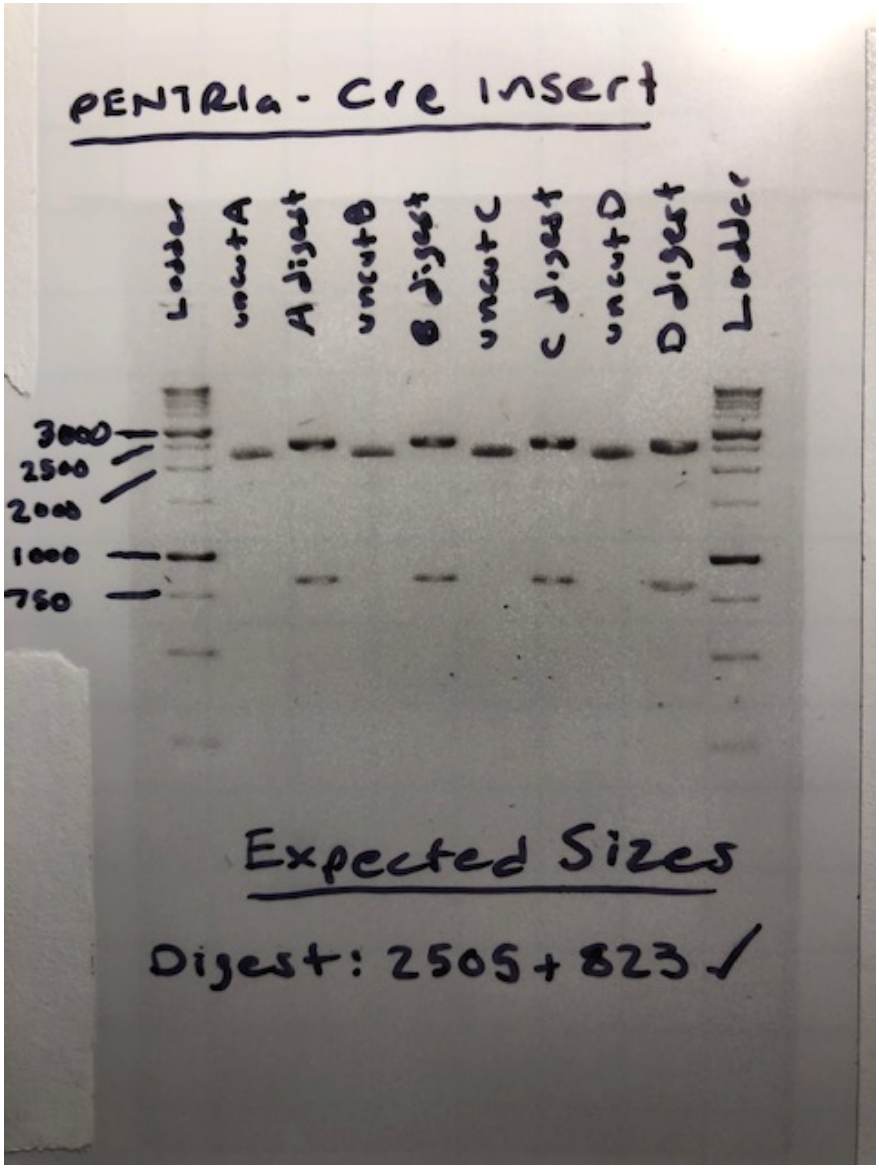

Figure S6: *cre* Ligation
Following the ligation of *cre* into the empty middle entry clone, this gel was ran in order to confirm proper ligation. Expected product sizes of digested ligation: 2505 bp, 823 bp.

V: References

1. Gilboa, Suzanne M., et al. “Congenital Heart Defects in the United States: Estimating the Magnitude of the Affected Population in 2010.” *Circulation*, vol. 134, no. 2, July 2016, pp. 101–109.
2. Kucik, James E., et al. “Racial/Ethnic Variations in the Prevalence of Selected Major Birth Defects, Metropolitan Atlanta, 1994-2005.” *Public Health Reports*, vol. 127, no. 1, Jan. 2012, pp. 52–61.
3. Fishman, M C, and K R Chien. “Fashioning the vertebrate heart: earliest embryonic decisions.” *Development (Cambridge, England)* vol. 124,11 (1997): 2099-117.
4. Moreno-Rodriguez, R A et al. “Bidirectional fusion of the heart-forming fields in the developing chick embryo.” *Developmental dynamics : an official publication of the American Association of Anatomists* vol. 235,1 (2006): 191-202. doi:10.1002/dvdy.20601
5. Mohun, T, and D Sparrow. “Early steps in vertebrate cardiogenesis.” *Current opinion in genetics & development* vol. 7,5 (1997): 628-33. doi:10.1016/s0959-437x(97)80010-x
6. Bussmann, Jeroen, et al. “Early Endocardial Morphogenesis Requires Scl/Tal1.” *PLoS Genetics*, vol. 3, no. 8, Aug. 2007, pp. 1425–1437.
7. Holtzman, Nathalia Glickman, et al. “Endocardium Is Necessary for Cardiomyocyte Movement during Heart Tube Assembly.” *Development (09501991)*, vol. 134, no. 12, June 2007, p. 18.

8. Le A. Trinh, and Didier Y. R. Stainier. “Fibronectin Regulates Epithelial Organization during Myocardial Migration in Zebrafish.” *Developmental Cell*, vol. 6, no. 3, Mar. 2004, p. 371.
9. Jackson, Timothy R., et al. “Spatiotemporally Controlled Mechanical Cues Drive Progenitor Mesenchymal-to-Epithelial Transition Enabling Proper Heart Formation and Function.” *Current Biology*, vol. 27, no. 9, May 2017, pp. 1326–1335.
10. Baum, Buzz, et al. “Transitions between Epithelial and Mesenchymal States in Development and Disease.” *Seminars in Cell & Developmental Biology*, vol. 19, no. 3, June 2008, pp. 294–308.
11. Yu-Huan Shih, Alexey V. Dvornikov, Ping Zhu, Xiao Ma, Maengjo Kim, Yonghe Ding, Xiaolei Xu *Development* 2016 143: 4713-4722; doi: 10.1242/dev.139246
12. Ding Ye, et al. “Endoderm Convergence Controls Subduction of the Myocardial Precursors during Heart-Tube Formation.” *Development (09501991)*, vol. 142, no. 17, Sept. 2015, pp. 2928–2940.
13. Varner, Victor D., and Larry A. Taber. “Not Just Inductive: A Crucial Mechanical Role for the Endoderm during Heart Tube Assembly.” *Development (09501991)*, vol. 139, no. 9, May 2012, pp. 1680–1690.
14. Alexander, J et al. “casanova plays an early and essential role in endoderm formation in zebrafish.” *Developmental biology* vol. 215,2 (1999): 343-57. doi:10.1006/dbio.1999.9441

15. Ye, Ding, and Fang Lin. “S1pr2/Gα13 Signaling Controls Myocardial Migration by Regulating Endoderm Convergence.” *Development (09501991)*, vol. 140, no. 4, Feb. 2013, pp. 789–799.
16. David, N B, and F M Rosa. “Cell autonomous commitment to an endodermal fate and behaviour by activation of Nodal signalling.” *Development (Cambridge, England)* vol. 128,20 (2001): 3937-47.
17. Lough, J, and Y Sugi. “Endoderm and heart development.” *Developmental dynamics : an official publication of the American Association of Anatomists* vol. 217,4 (2000): 327-42. doi:10.1002/(SICI)1097-0177(200004)217:4<327::AID-DVDY1>3.0.CO;2-K
18. Bloomekatz, Joshua, et al. “Platelet-Derived Growth Factor (PDGF) Signaling Directs Cardiomyocyte Movement toward the Midline during Heart Tube Assembly.” *ELife*, Jan. 2017, pp. 1–23.
19. Andrae, Johanna, et al. “Role of Platelet-Derived Growth Factors in Physiology and Medicine.” *Genes & Development*, vol. 22, no. 10, May 2008, pp. 1276–1312.
20. Ataliotis, P et al. “PDGF signalling is required for gastrulation of Xenopus laevis.” *Development (Cambridge, England)* vol. 121,9 (1995): 3099-110.
21. Schatteman, G C et al. “Platelet-derived growth factor receptor alpha subunit deleted Patch mouse exhibits severe cardiovascular dysmorphogenesis.” *Teratology* vol. 51,6 (1995): 351-66. doi:10.1002/tera.1420510602
22. Tallquist, Michelle D, and Philippe Soriano. “Cell autonomous requirement for PDGFRalpha in populations of cranial and cardiac neural crest cells.”

Development (Cambridge, England) vol. 130,3 (2003): 507-18. doi:10.1242/dev.00241

23. Bleyl, Steven B et al. "Dysregulation of the PDGFRA gene causes inflow tract anomalies including TAPVR: integrating evidence from human genetics and model organisms." *Human molecular genetics* vol. 19,7 (2010): 1286-301. doi:10.1093/hmg/ddq005
24. Smith, Christopher L et al. "Epicardial-derived cell epithelial-to-mesenchymal transition and fate specification require PDGF receptor signaling." *Circulation research* vol. 108,12 (2011): e15-26. doi:10.1161/CIRCRESAHA.110.235531
25. Richarte, Alicia M., et al. "Cooperation between the PDGF Receptors in Cardiac Neural Crest Cell Migration." *Developmental Biology*, vol. 306, no. 2, June 2007, pp. 785–796.
26. Pan, Xiufang et al. "Demonstration of site-directed recombination in transgenic zebrafish using the Cre/loxP system." *Transgenic research* vol. 14,2 (2005): 217-23. doi:10.1007/s11248-004-5790-z
27. Pang, Shao-Chen et al. "Transcriptional Activity and DNA Methylation Dynamics of the Gal4/UAS System in Zebrafish." *Marine biotechnology (New York, N.Y.)* vol. 17,5 (2015): 593-603. doi:10.1007/s10126-015-9641-0
28. Köster, R W, and S E Fraser. "Tracing transgene expression in living zebrafish embryos." *Developmental biology* vol. 233,2 (2001): 329-46. doi:10.1006/dbio.2001.0242

29. Sauer, B. “Functional expression of the cre-lox site-specific recombination system in the yeast Saccharomyces cerevisiae.” *Molecular and cellular biology* vol. 7,6 (1987): 2087-96. doi:10.1128/mcb.7.6.2087

30. Howe, Kerstin, et al. “The Zebrafish Reference Genome Sequence and Its Relationship to the Human Genome.” Nature, vol. 496, no. 7446, Apr. 2013, pp. 498–503.

31. Meyers, J. R. (2018). Zebrafish: Development of a vertebrate model organism. *Current Protocols Essential Laboratory Techniques*, e19. doi: 10.1002/cpet.19

32. Kimmel, C B et al. “Stages of embryonic development of the zebrafish.” *Developmental dynamics : an official publication of the American Association of Anatomists* vol. 203,3 (1995): 253-310. doi:10.1002/aja.1002030302

33. Hu, N et al. “Structure and function of the developing zebrafish heart.” *The Anatomical record* vol. 260,2 (2000): 148-57. doi:10.1002/1097-0185(20001001)260:2<148::AID-AR50>3.0.CO;2-X

34. Vornanen, Matti, and Minna Hassinen. “Zebrafish heart as a model for human cardiac electrophysiology.” *Channels (Austin, Tex.)* vol. 10,2 (2016): 101-10. doi:10.1080/19336950.2015.1121335

35. Chi, Neil C., et al. “Genetic and Physiologic Dissection of the Vertebrate Cardiac Conduction System.” *PLoS Biology*, vol. 6, no. 5, May 2008, p. e109.